Universidad Popular Autónoma del Estado de Puebla

DEPARTMENT OF BIOLOGICAL SCIENCES

"Ag nanoparticles biosynthesis using water hyacinth (*Eichnornia crassipes*) as reductant agent"

THESIS

To obtain the title of:

Engineer in biotechnology

Presents:

ARELI MUNIVE OLARTE

Advisors:

PhD. GENOVEVA ROSANO ORTEGA

PhD. PABLO SAMUEL SCHABES RETCHKIMAN

M.S. MARIA CRISTINA MIRANDA VERGARA

Puebla, Pue., México

30 May, 2014

Declaration of Authorship

I, Areli Munive Olarte, declare that this thesis titled, "Ag nanoparticles biosynthesis using water hyacinth *(Eichnornia crassipes)* as reductant agent" and the work presented in it are my own. I confirm that:

- This work was done wholly or mainly while in candidature for a research degree at this University.
- Where I have consulted the published work of others, this is always clearly attributed.
- Where I have quoted from the work of others, the source is always given. With the exception of such quotations, this thesis is entirely my own work.
- I have acknowledged all main sources of help.
- Where the thesis is based on work done by myself jointly with others, I have made clear exactly what was done by others and what I have contributed myself.

Signed: _____

Date: _____

Abstract

There is a growing need to develop eco-friendly benign metal nanoparticle synthesis process that do not use toxic chemicals in the synthesis protocols to avoid adverse effects in medical applications. Here, it is a report on extracellular synthesis method for the preparation of silver nanoparticles using water hyacinth, an aquatic invasive plant, collected for the reservoir Manuel Avila Camacho. Ag, AgO and Ag2O3 at different sizes (<1-80 nm) characterized with transmission electron microscopy (TEM); were formed by treating an aqueous Ag2NO3 solution using root, stem or leaf as reducing agent, and varying pH. Uv-visible spectroscopy was used for measured absorption and identify silver surface plasmon band. Particle size distribution were measure with Dynamic Light Scattering (DLS) and the results were compared with TEM particle analysis. According to Fourier-transform infrared spectroscopy (FTIR), the possible biomolecules responsible for capping Ag nanoparticles are some proteins and metabolites such as tannins, terpenoids having functional groups of amines, alcohols, ketones, aldehydes, and carboxylic acids.

Acknowledgements

I would like to thank to my advisors Ph.D Genoveva Rosano Ortega, Ph.D. Pablo Samuel Schabes Retchkiman and MS Maria Cristina Miranda Vergara for their valuable guidance and extraordinary support in this thesis process. I offer my sincere appreciation for the learning opportunities provided by my advisors.

My completion of this project could not have been accomplished without the support of Ph.D Gustavo Hirata Flores, Ph.D Miguel ´Angel M´endez Rojas, Ph.D Hugo Tiznado V´azquez, Ph.D Mauricio Ortiz Guti´errez, Ph.D Alan **Augusto Gallejos Cuellar,** and MS Marcos Bedolla **Hernández**; thank you for allowing me time away from your research.

I wish to thank my parents for their full support and interest, who inspired me and encouraged me to go my own way, without whom I would be unable to complete my project. At last but not the least I want to thank my friends who appreciated me for my work and motivated me.

Contents

List of Figures

List of Tables

Dedicated to my parents and grandfather

Introduction

Biosynthesis of nanoparticles has become an important area of research in nanotechnology as an emerging point of intersection between nanotechnology and biotechnology. Due to the growing need to develop technology friendly to the environment [87], using organisms (bacteria, fungi and plants) [88]; which concerns the synthesis of nanoparticles of different chemical composition, sizes and shapes [97].

Because of their small size, nanoparticles show unique physical and chemical properties, such as: color, melting temperature, crystal structure, chemical reactivity, electrical conductivity, magnetism, mechanical strength,etc; that are different compared to the bulk material [13], [101]. Moreover, the nanoparticles show bactericidal effects. These essential qualities have been attributed to silver nanoparticles (AgNPs). Therefore, in nano-biotechnological research, AgNPs have received significant attention because of their unique physical, chemical, biological properties, and because of their applicability in electronics, optics and medicine [44].

We are reporting the synthesis of silver nanoparticles with water hyacinth (*Eichnornia crassipes*) evaluating the influence of three variables (pH, metal concentration, plant section) on the size and structure of these. The size, composition and structure of the synthesized nanoparticles were measured using ultraviolet visible spectroscopy (UV-Vis), dynamic light scattering (DLS), transmission electron microscopy (TEM) and high resolution (HRTEM), energy dispersive spectroscopy ray X (EDS), and Fourier transform infrared spectroscopy (FT-IR).

Problem Description

Generally silver nanoparticles are synthesized by various methods whether physical or chemical such as: radiolytic, photochemical, sonochemical, [73] [34] thermal decomposition in organic solvents, chemical reduction [115], photoreduction in reverse micelles, radiation chemical reduction [46], sol-gel methods, etc.; that need controlled environments, and sometimes the chemicals used in the synthesis and stabilization are toxic and expensive and give rise to non-organic products [46], [34]. That is why there is a need to create protocols for a synthesis based on Green Chemistry that operate in water, a benign solvent [33]. Particularly in biomimetic synthesis, one of the fundamental processes is bioreduction; biological methods of nanoparticles synthesis using microorganism, enzymes, fungus, and plants [46]. The plants were observed to be a good source for the synthesis of nanoparticles, where the variability of size and shape can be induced by varying the pH [28], [102]. Nanoparticles produced by plants are more stable, economical and the rate of synthesis is faster than in the case of microorganisms [46], [85]. Plant extracts from live alfalfa, the broths of lemongrass, geranium leaves and others have served as green reactants in Ag NP synthesis, but most of the plants used to synthesized metal nanoparticles form part of the human or animal diet, or are specific to a certain region.

In this research we are proposing a new alternative of a reducing agent for the synthesis of silver nanoparticles. The synthesis method proposed here was first developed by G. Rosano et al. 2006, that make use of water hyacinth (*Eichhornia crassipes*). Water hyacinth is one of the world's worst aquatic weeds [37], which grow in all types of freshwater lakes, rivers, ponds, ditches of temperate climates [45]. This plant causes eutrophication in aquatic systems because it reduces the levels of dissolved oxygen in water bodies, thereby altering the structure and function of the ecosystem by disruption of food chains and nutrient cycling,

encouraging growth of other aquatic species. Being a plant of high growth, decomposition leads to deterioration of the quality of fresh water, threatening human health and reducing fish production [7], [112]; large amounts of waste organic matter is also produced, which involves a high cost to perform cleanup actions at the reservoir. This generates the opportunity of using this plant as raw material in the bioreduction method described, obtaining environmental, economic and social benefits [111].

This Thesis aims to provide information and respond to the educational community in relation to the following question: What are the synthesis conditions to obtain Ag nanoparticles $\leq$ 10nm using water hyacinth as a reducing agent? The research question proposed seeks the relationship between the following three parameters of synthesis: 1) section of the plant, 2) pH, 3) metal concentration. The background described in the following paragraphs sustained the approach to the problem of the present investigation.

Project Justification

The synthesis and application of water-soluble Ag nanoclusters is not an emerging research area [115]. Over the last century, products containing nanoscale silver have been commercially available and used in diverse applications such as pigments, photography, wound treatment, conductive/autostatic composites, catalysts, and as a biocide. Silver's antibacterial qualities have applications that reach far beyond the medical world. Washing machines, refrigerators, air conditioners, air purifiers and vacuum cleaners all rely upon silver nanoparticles to sterilize up to 650 types of bacteria [113]. It is estimated that today about 320 tons/year of nanosilver are produced and used worldwide [50]. Over the last 15 years, Food and Drug Administration (FDA) granted 510(k) approval to dozens of products containing nanosilver to prevent colonization on various surfaces, including wound dressings, catheters and topical gels [59].

This project is going to develop a self-sustaining method to synthesized silver nanoparticles for commercial use, where biomass as a reducing agent, comes from an aquatic weed obtained from the Valsequillo reservoir located at Puebla.

For the characterization of nanoparticles, we have the collaboration of Institute of Physics at the UNAM; of the Center for Nanoscience and Nanotechnology at the UNAM, of the Department of Chemical and Biological Sciences at UDLAP, the School of Physical Mathematical Sciences at UMICH, and by the Department of Biological Sciences and Research Department at UPAEP.

Objectives

Main Objective

To evaluate biorreduction method using water hyacinth (*Eichnornia crassipes*), plant considered as plague in Manuel Ávila Camacho reservoir located in Puebla state, for Ag nanoparticles synthesis in the quantum dots scale (nanopartices $<$ 10nm), evaluating the influence of pH, concentration of metal, and part of the plant (root, stem, leaf) in their size and structure.

Particular Objectives

1.- Make an instantaneous representative sampling of water hyacinth (*Eichnornia crassipes*) from Manuel Ávila Camacho reservoir located in Puebla, based on criteria established under NMX-AA-014-1980, for biomass procurement as a reducing agent in the method.
2.- Condition water hyacinth through wash, dry and powder, to obtain active dehydrated biomass.
3.- Optimize biorreduction method developed by G. Rosano et al. 2006 in Ag nanoparticles, modifying synthesis conditions to simplify operations with a field manipulation perspective.
4.- Characterize Ag nanoparticles through spectrometry techniques (UV-Visible, Dynamic Light Scattering) and microscopy (Transmission Electron Microscopy), to establish size and structure of the nanoparticles.
5.- Characterize by Fourier transform infrared spectroscopy the possible biomolecules responsible for capping of Ag nanoparticles.

Hypothesis

It is possible to obtain Ag quantum dots (nanoparticles < 10nm) in its basal state, with a homogeneous size distribution through the implementation of a synthesis method of bioreduction using *Eichnornia crassipes* (water hyacinth).

Research Limitations

This project has some limitations, concerning to:

- Physical-geographic space: in this project, complexity came from the use of most of the instruments or techniques of measurement because: a) the high demand, b) location, c) waiting list. Another problem has been the interpretation of the data, and experts of the area are far away; so the communication has been complicated because of the distance and even different schedule.

- Time: the physical measurements were done at bit late, because of the difficulties mentioned above.

- Resources:the support was good but not favorable to do the physical measurements on time.

- Personal: there are some proficiency limitations, which limited me to analyze and to interpret some data.

Chapter 1

Background

1.1 Nanotechnology

This chapter gives an introduction to the subject of nanotechnology, relevance and applications. To metal nanoparticles, properties, methods of synthesis, characterization, and finally some applications.

Defining Nanotechnology

The term was first coined in 1974 by a Japanese physicist professor Norio Taniguchi, who used it to describe the processes of creating semiconductor structures with nanometer precision using the focused ion beam technique, atomic layer deposition and other methods. Taniguchi wrote, "Nanotechnology mainly consists of the processes of separation, consolidation, and deformation of materials by one atom or one molecule". Over a decade later, the term without the knowledge of Norio Taniguchi, was popularized by an American engineer K. Eric Drexler[40],[94]. He writes the first journal article discussing "nanotechnology". His article, entitled "Molecular Engineering: An approach to the development of general capabilities for molecular manipulation", was published in 1981 in the journal *Proceedings of the National Academy of Sciences*. Dexler was stimulated by Molecular Biology, to him life was the existence proof that machines could be designed and built atom by atom. His argument was the idea of a Universal Assembler, he was talking about building machines on the scale of molecules[41].

Since its inception, the National Nanotechnology Initiative (NNI) has defined "nanotechnology" as encompassing the science, engineering, and technology related to the understanding and control of matter at the length scale of approximately 1 to 100 nanometers. As used today, the meaning of the word shifted to encompass diverse fields; multiple published definitions are given, from which do not exist a consensus. However, nanotechnology is not merely working with matter at the nanoscale, but also research and development of materials, devices, and systems that have novel properties and functions due to their nanoscale dimensions or components [5].

Relevance and Applications

Nanotechnology involves a new and broad science where diverse fields such as physics, chemistry, biology, materials science, and engineering converge at the nanoscale. After more than 20 years of basic nanoscience research and more than a decade of focused R&D under the NNI, applications of nanotechnology are delivering in both expected and unexpected ways on nanotechnology's promise to benefit society. It will offer better built, longer, lasting, cleaner, safety and smaller products for the house, communications, medicine, transportation, agriculture and industry in general [56].

Although nanotechnology is a relatively new field, the economic support to this area reflects a global interest because of its potential [76].The global market for nanotechnology was valued at nearly $20.1 billion in 2011 [93]. The 2014 Federal Budget provides more than $1.7 billion for the National Nanotechnology Initiative (NNI), reflecting steady growth in the NNI investment. The cumulative NNI investment since fiscal year 2001, until the 2014 request, now totals almost $20 billion. Cumulative investments in nanotechnology-related environmental, health, and safety research since 2006 now total nearly $750 million [56].

Widespread commercial adoption of nanotechnology is growing rapidly. Examples of areas in which nanotechnology is expected to have a high commercial impact include [35]:

• Near-term (1-5 years):
Long-lasting rechargeable batteries
Improved chemical & biological sensors

Point-of-care medical diagnostic devices

• Mid-term (5-10 years):
New targeted drug therapies
Enhanced medical imaging
High-efficiency, cost-effective solar cells

• Long-term (20+ years):
New molecular electronics
New all-optical information processing
New neural prosthetics for health care

1.2 Metal Nanoparticles

Nanoparticles (NPs) are clusters of atoms, ions or molecules, with dimensions of 1-20nm. This is a particularly engaging size range, which bridges the gap between small molecules and bulk materials. NPs can be formed by most of the elements in the periodic table; metallic elements form a wide variety of them and may be composed of a single metallic element or more than one metal[114]. Metal nanoclusters exhibit unusual chemical and physical properties different from those of the bulk material or of the atoms [31], for example:

• Nanosize transition metal clusters melt at much lower temperature than the bulk metal; the melting temperature depends on cluster size, shape, and chemical composition.

• Wetting behavior (island formation on the substrate) can be induced by thermal treatments or by substrate chemical and physical modifications.

• Bimetallic systems that exhibit surface segregation behavior melt in two stages: surface diffusion followed by total melting.

Why metal nanoparticles are so attractive in biotechnology?
In general, NPs used in the field of biotechnology range in particle size between 10

and 500 nm. The nanosize of these particles allows various communications with biomolecules on the cell surfaces and within the cells in a way that can be decoded and designated to various biochemical and physicochemical properties of these cells. Its potential application in drug delivery systems and noninvasive imaging offered various advantages over conventional pharmaceutical agents. It is important that nanosystems should be stable, biocompatible, and selectively directed to specific sites in the body after systemic administration. More specific targeting systems are designed to recognize the targeted cells such as cancer cells. This can be achieved by conjugating the nanoparticle with an appropriate ligand, which has a specific binding activity with respect to the target cells. These advances in the field of biotechnology have opened an endless opportunities for molecular diagnostics and therapy [77].

1.3 Silver Nanoparticles

In its bulk form, Ag is a naturally occurring, soft, white, lustrous, transition metal. Every use of Ag has matured and continued over thousands of years, varying in function from jewelry and currency, to dental alloys, tableware, electrical wiring and as antimicrobial agent. Ag has the highest electrical conductivity of any element and the highest thermal conductivity of any metal. Along this line, ionic silver has a long history and was initially used to stain the glass like gold nanoparticles. The augmented properties of Ag at nanoscale were in the fields of spectroscopy and physics, owing to their remarkable surface plasmon [95].

Properties

Ag-NPs have distinctive physical-chemical properties, including a high electrical and thermal conductivity, surface-enhanced Raman scattering, chemical stability, catalytic activity and non linear optical behavior. Besides, Ag-NPs exhibit broad spectrum bactericidal and fungicidal activity[90].

Thermodynamic properties

It has been well established both experimentally and theoretically that the melting temperature of nanoparticles depends on the particle size. However, Pawlow in

1909 developed a thermodynamic model that predicts a melting point depression of nanoparticles. The isolated nanoparticles and substrate-supported nanoparticles exhibit a significant decrease in melting temperature as compared with the corresponding conventional bulk materials with anomaly in few cases [78]. The physical origin for this phenomenon is that nanoparticles possess a very high surface to volume ratio [83] Therefore, as the particle size decreases, its surface-to-volume atom ratio increases and the melting temperature decreases as a consequence of the improved free energy at the particle surface [90].

Antimicrobial effects

There is a strong need to develop new bactericides and virucides, due to the resistance to medication shown by pathogens[54]. It is well known that silver ions are highly toxic to microorganisms showing strong biocidal effects on as many as 16 species of bacteria [105] including multi-resistant bacteria like Methicillin-resistant Staphylococcus aureus (MRSA), as well as multidrug-resistant Pseudomonas aeruginosa, ampicillin-resistant E. coli O157:H7 and erythromycin-resistant S. pyogenes. The mechanism of inhibitory action of silver ions on microorganism is not completely clear. It is believe that DNA loses its replication, inhibitory growth, ability and cellular proteins become inactivated on Ag+ treatment, also it binds to functional groups of proteins, resulting in protein denaturation. The shape, size, concentration of AgNPs and the sensitivity of the microbial species to silver are factors to the effectivity to cell death [54].

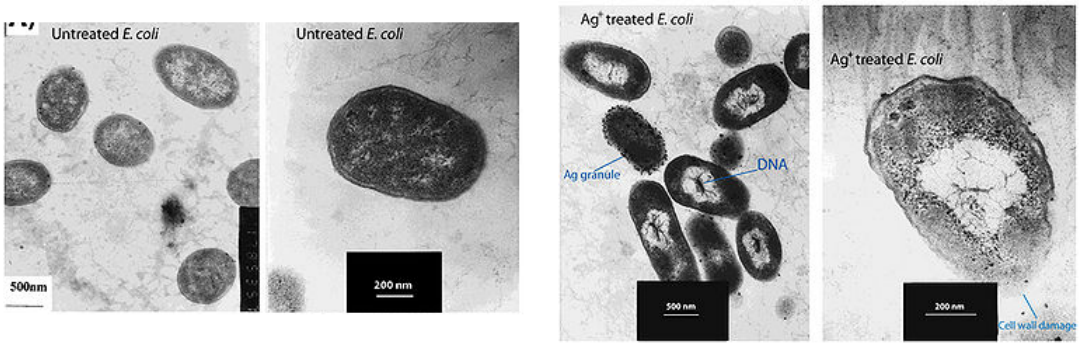

FIGURE 1.3.1: Treatment of cells with Ag+ results in DNA condensation, cell wall damage, and silver granule formation. E. coli cells with and without Ag+ treatment were observed with transmission electron microscopy (Feng et al., 2000)

Applications

Silver nanoparticles have unique optical, electrical, and thermal properties and are being incorporated into products that range from photovoltaics to biological and chemical sensors (fluorescent nanotags). Examples include conductive inks, pastes and fillers which utilize silver nanoparticles for their high electrical conductivity, stability, and low sintering temperatures. Additional applications include molecular diagnostics and photonic devices (data storage device, photovoltaic cells) which take advantage of the novel optical properties of these nanomaterials. An increasingly common application is the use of silver nanoparticles as anti-bacterial agents in the health industry, food storage, textile coatings, environmental applications (Air disinfection,water desinfection, Groundwater and biological wastewater disinfection) many textiles, wound dressings, and biomedical devices (Figure 1.3.2) [106], [19], [90].

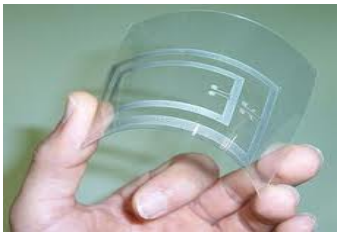

(A) Conductive films

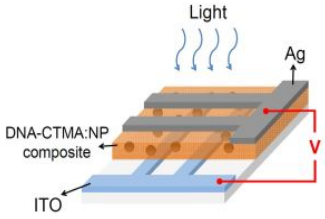

(B) Data Storage Device

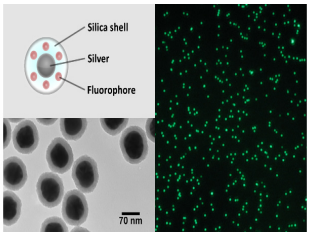

(C) Fluorescent Nanotags

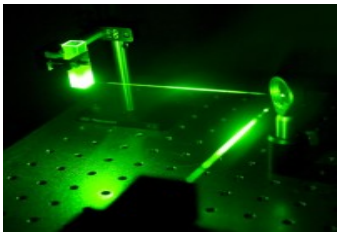

(D) Molecular Detection

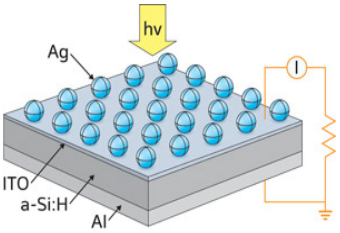

(E) Solar cell

(F) Socks

FIGURE 1.3.2: Applications of silver nanoparticles

1.4 Synthesis methods

The methods for nanoparticle synthesis are described in this section. The nanoparticle synthesis methods can be divided into two approaches: "top-down" and "bottom-up" [38], [92].

Top-down methods

In the "top-down" approach it all begins from a bulk piece of material, which is then gradually or step by step removed to form objects in the nanometer size (1x10-9 m)[38]. This approach may involve milling, chemical methods, and the volatilization of a solid followed by the condensation of the volatilized components [117]. At the nanoscale though, these methods are generally not suitable for production on a very large scale because they presently encounter technological limitation and require extremely long and costly processes [38]. Here, we are going to describe only the most common methods.

Nanolitography

Nanolithography derives its name from the Greek words nanos (dwarf), lithos (rock), and grapho (to write), which literally means "small writing on rocks" [38], [91]. Nanolithography is the branch of nanotechnology concerned with the study and application of the nanofabrication of nanometer-scale structures, meaning nanopatterning with at least one lateral dimension between the size of an individual atom and approximately 100 nm. Nanolithography is used e.g. during the nanofabrication of leading-edge semiconductor integrated circuits (nanocircuitry), for nanoelectromechanical systems (NEMS) or for almost any other fundamental application across various scientific disciplines in nanoresearch [91]. Lithography can be performed using light (optical- or photolithography), electrons (e-beam lithography), ions (i-beam lithography), or X-ray (X-ray lithography, LIGA) depending on the desired minimum feature size of the outputs [38].

Photolithography

Optical Lithography refers to a lithographic process that uses visible or ultraviolet light to form patterns on the photoresist through printing. Printing is the process of projecting the image of the patterns onto the wafer surface using a light source and a photo mask [103].

The lens is used to focus the sectioned UV light down to a smaller area on the chip. The smallest feature size capable of being written on the wafer is a function of the numerical aperture of the lens as well as the wavelength of the light [80].

E-beam lithography

Electron Beam Lithography (EBL) refers to a lithographic process that uses a focused beam of electrons to form the circuit patterns needed for material deposition on (or removal from) the wafer, in contrast with optical lithography which uses light for the same purpose. Electron lithography offers higher patterning resolution than optical lithography because of the shorter wavelength possessed by the 10-50 keV electrons that it employs. A typical EBL system consists of the following parts: 1) an electron gun or electron source that supplies the electrons; 2) an electron column that 'shapes' and focuses the electron beam; 3) a mechanical stage that positions the wafer under the electron beam; 4) a wafer handling system that automatically feeds wafers to the system and unloads them after processing; and 5) a computer system that controls the equipment [104].

I-beam lithography

Ion-beam lithography commonly uses light ions (protons, helium ions) for the exposure of polymeric resists. The use of heavier ions makes it possible to dope the substrate or create thereon thin layers of new chemical compounds. Differences between the electron and ion lithography are due to greater mass of an ion as compared to the mass of an electron and to the fact that an ion is a many-electron system. A thin beam of ions has a weaker angular scattering in the target than an electron beam, therefore ion-beam lithography has a higher resolution than electron beam lithography [55].

X-ray lithography

Optical lithography is limited by diffraction, which is mos significant when objects are comparable in size to the wavelength of light. This fact of physics has driven decreases in the wavelength of light used in optical lithography. Similarly, the use for lithography of wavelength in the x-ray portion of the electromagnetic spectrum was motivated by the idea that diffraction effects could be effectively neutralized by using photons with extreme short wavelengths [70].

Thermal Evaporation (PVD)

Thermal evaporation is a process wherein a solid material is heated inside a high vacuum chamber to a temperature which generates some vapor pressure. Inside the vacuum, even a very low vapor pressure is adequate to create a vapor cloud

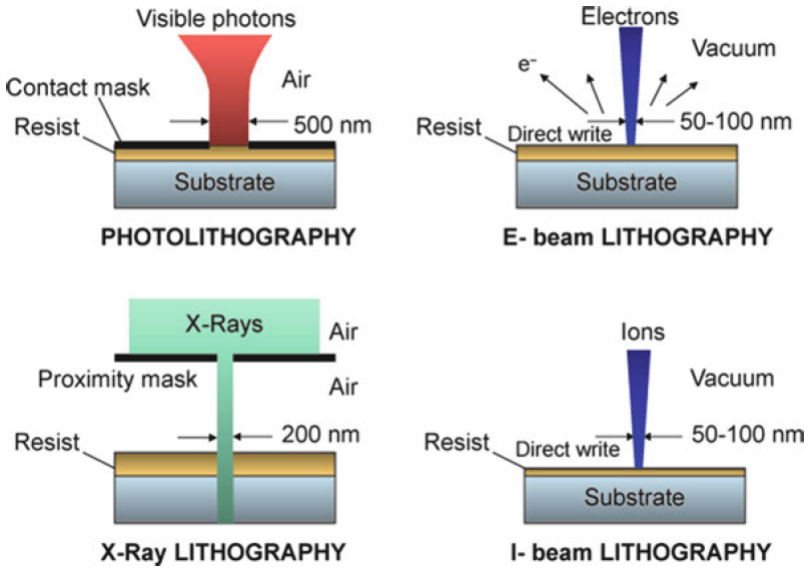

FIGURE 1.4.1: Comparison of the described lithography techniques

within the chamber. This evaporated material now consists of a vapor stream, which passes through the chamber, and strikes and sticks onto the substrate as a film or coating. Since, in a majority of cases, the material becomes liquid by heating it to its melting temperature, it is normally placed in the bottom of the chamber, often in some form of upright crucible. The vapor then rises above from this bottom source and reaches the substrates that are held inverted in suitable fixtures at the top of the chamber, with surfaces to be coated facing down toward the rising vapor to acquire their coating [30].

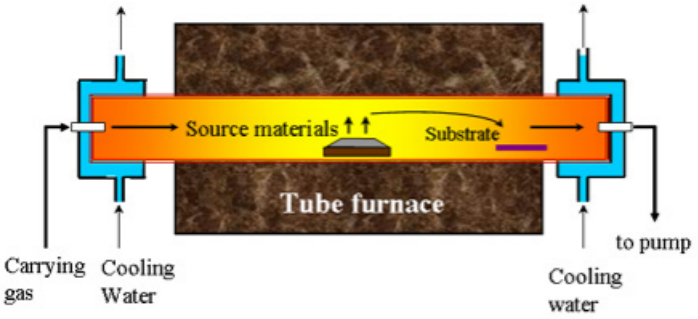

FIGURE 1.4.2: Thermal evaporate deposition system for synthesis of 1D nanostructures

Various measures may have to be taken in order to ensure film adhesion and control different film properties as desired. The evaporation system design allows process engineers to adjust a number of parameters to obtain desired results for variables such as grain structure, uniformity, thickness, stress, adhesion strength,

optical or electrical properties, and much more[30].
PVD comprises the standard technologies for deposition of metals. It is far more common than CVD for metals since it can be performed at lower process risk and cheaper in regards to materials cost. The quality of the films are inferior to CVD, which for metals means higher resistivity and for insulators more defects and traps. The step coverage is also not as good as CVD [74].

Bottom-up methods

The "bottom-up" approach on the other hand takes the idea of "top-down" approach and flips it right over. In this case, instead of starting with large materials and chipping them away to reveal small bits of them, it all begins from atoms and molecules that get rearranged and assembled to larger nanostructures [38]. Consists on the manufacture of nanoparticles through the condensation of atoms or molecular entities in a gas phase or in solution. Nanoparticles can be supported or noT. The support gives stability to the nanoparticles, also it can give them specific properties [117].

Chemical Vapor Deposition (CVD)

In this process, the substrate is placed inside a reactor to which a number of gases are supplied. The fundamental principle of the process is that a chemical reaction takes place between the source gases. The product of that reaction is a solid material with condenses on all surfaces inside the reactor [74].
CVD processes are ideal to use when you want a thin film with good step coverage. A variety of materials can be deposited with this technology, however, some of them are less popular with fabs because of hazardous byproducts formed during processing. The quality of the material varies from process to process, however a good rule of thumb is that higher process temperature yields a material with higher quality and less defects [74].

Chemical Vapor Synthesis

Chemical Vapor Synthesis (CVS) is a modified Chemical Vapor Deposition (CVD) method where the process parameters are adjusted to form nanoparticles instead of film [39]. The entire range of reaction regimes and corresponding microstructures (epitaxial, polycrystalline, columnar, granular films and aerogel coatings as well as nanopowders) are shown in thee figure 1.4.3.

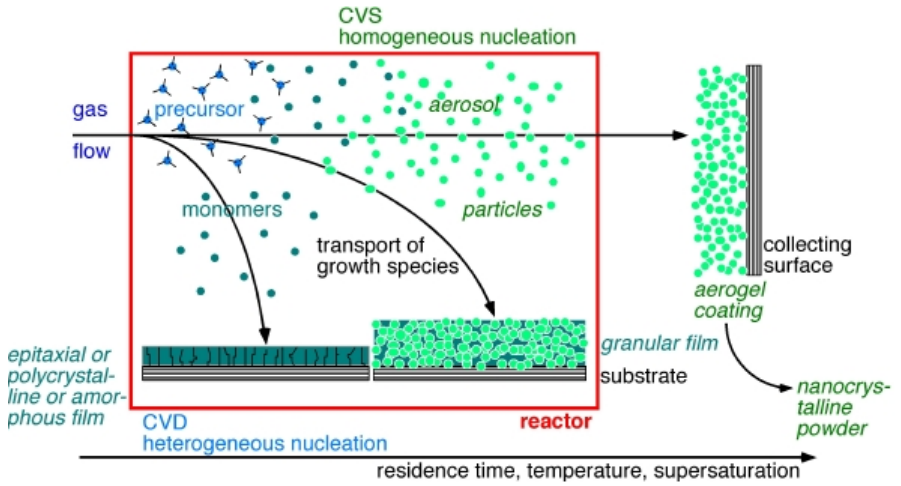

FIGURE 1.4.3: Comparison between CVD and CVS techniques

Both in CVD and CVS, precursors are metalorganics, carbonyls, hydrides, chlorides and other volatile compounds in gaseous, liquid or solid state. The major limitation of the CVS process is the availability of appropriate precursor materials. The energy for the conversion of the reactants into nanoparticles is supplied in hot wall (external furnace), flame (reaction enthalpy), plasma (microwave or radio frequency) and laser (photolysis or pyrolysis) reactors. Chemical Vapor Reaction (CVR), Chemical Vapor Condensation (CVC), Chemical Vapor Precipitation (CVP) are synonyma used frequently in the literature. The most important process parameters determining the quality and usability of the nanopowders are the total pressure (typical range from 100 to 100000 Pa), the precursor material (decomposition kinetics and ligands determining the impurity level), the partial pressure of the precursor (determining the production rate and particle size), the temperature or power of the energy source, the carrier gas (mass flow determining the residence time) and the reactor geometry. The nanoparticles are extracted from the aerosol by means of filters, thermophoretic collectors, electrostatic precipitators or scrubbing in a liquid [39].

Colloidal Chemistry

Colloids are individual particles, which are larger than the dimensions atomic, but small enough to exhibit Brownian motion. If the particles are large enough, then their dynamic behavior in suspension in function of time is governed by gravity and sedimentation will occur. If the particles are enough small to be colloids, then their irregular motion in suspension can be attributed for collective bombings by a multitude of thermally agitated molecules in a liquid suspension. This range of

size of particles in a solution colloidal usually varies in the range of nanometers, so the colloid method is an efficient method of producing nanoparticles. This method consists in dissolving a precursor of the metal salt or oxide, a reducer and a stabilizer in a continuous phase. The average size, size distribution, shape and morphology of the nanoparticles can be controlled by varying the concentration of the reactants [118].

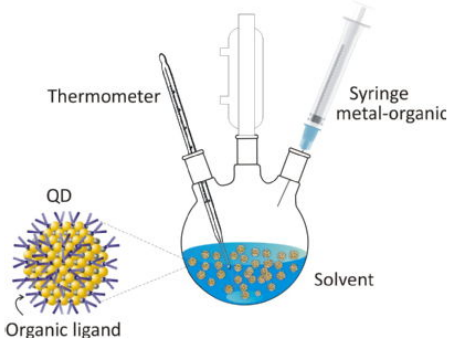

FIGURE 1.4.4: A schematic of a three neck flask used in the preparation of colloidal QDs

The main problems are reproducibility between batches and producing particles in large quantities. Another important barrier is finding the appropriate surfactant that will eliminate agglomeration of the nanoparticles. Environmental problems identified for the sol-gel approach are also applicable to this method [86].

Sol-gel

The sol-gel process, as the name implies, involves the transition of a solution system from a liquid "sol" (mostly colloidal) into a solid "gel" phase [89]. The precursors for synthesizing these colloids consist usually of a metal or metalloid element surrounded by various reactive ligands. The starting material is processed to form a dispersible oxide and forms a sol in contact with water or dilute acid. Removal of the liquid from the sol yields the gel, and the sol/gel transition controls the particle size and shape [110]. Utilizing the sol-gel process, it is possible to fabricate advanced materials in a wide variety of forms: ultrafine or spherical shaped powders, thin film coatings, fibers, porous or dense materials, and extremely porous aerogel materials [89].

There are difficulties in simultaneously controlling all parameters. For this reason, reproducibility is often an issue. In general, low yields are obtained by using the

sol-gel approach. Also, there are minor environmental problems, such as large volumes of contaminated solvent (usually water) to deal with [86].

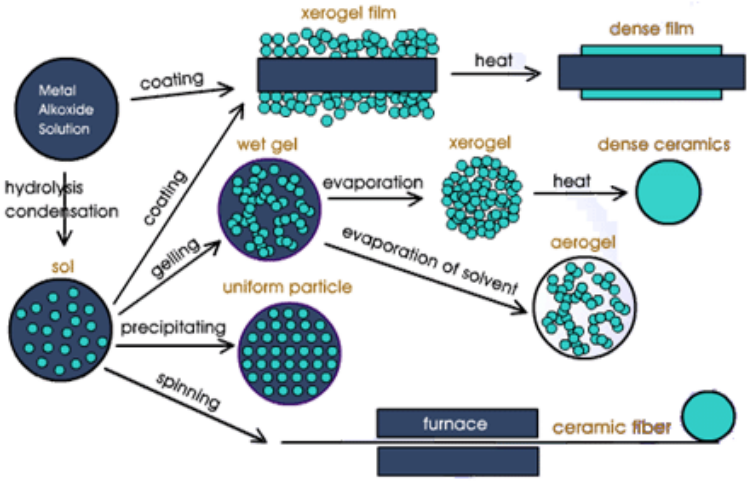

FIGURE 1.4.5: Schematic representation of the different stages and routes of the sol-gel technology

Molecular Self-Assembly

Molecular self-assembly is the assembly of molecules without guidance of managements from an outside source. Self-assembly can occur spontaneously in nature, for example, in cells such as the self-assembly of the lipid bilayer membrane. It usually results in an increase in the internal organization of the system [60].

In self-assembly, the final structure is "encoded" in the shape and properties of the molecules that are used, as compared to traditional techniques, such as lithography, where the desire final structure must be carved out to from a larger block of matter [60].

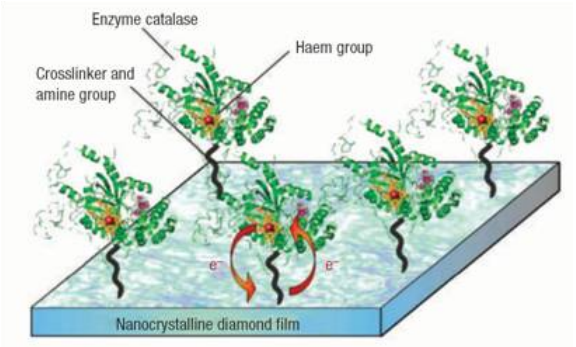

FIGURE 1.4.6: Prototype biosensor based on enzyme units anchored on a nanocrystalline diamond surface functionalized with a self-assembled monolayer (SAM) of spacer molecules

Biological Methods

Because, most of the methods mention above (top-down and bottom-up) are extremely expensive and they also involve the use of toxic, hazardous chemicals which may pose potential environmental and biological risks. A quest for an environmentally sustainable synthesis process has led to few biomimetic approaches. Biomimetics refers to applying biological principles in materials formation. One of the fundamental processes in the biomimetic synthesis involves bioreduction [4]. Living organism such as bacteria, fungi and plants have a huge potential for the production of metal nanoparticles [51]. The table 1.4.1 shows Au and Ag nanoparticles produced by some microorganisms.

TABLE 1.4.1: Metal nanoparticles synthesized by microorganisms

Microorganisms	Products	Size (nm)	Shape	Location	Reference
Sargassum wightii	Au	8–12	planar	Extracellular	[47]
Rhodococcus sp.	Au	5–15	spherical	Intracellular	[1]
Shewanella oneidensis	Au	10-17	spherical	Extracellular	[2]
Plectonemaboryanum	Au	< 10–25	cubic	Intracellular	[72]
Trichoderma viride	Ag	5–40	Spherical	Extracellular	[3]
Bacillus licheniformis	Ag	50	Not available	Extracellular	[63]
Escherichia coli	Ag	37	Not available	Extracellular	[23]
Corynebacterium glutamicum	Ag	5–50	Irregular	Extracellular	[18]
Trichoderma viride	Ag	2–4	Not available	Extracellular	[8]
Ureibacillus thermosphaericus	Au	50–70	Not available	Extracellular	[21]
Bacillus cereus	Ag	4-5	Spherical	Intracellular	[20]
Aspergillus flavus	Ag	8.92	Spherical	Extracellular	[22]
Aspergillus fumigatus	Ag	5-25	Spherical	Extracellular	[17]
Verticillium sp.	Ag	25	Spherical	Extracellular	[24]
Fusarium oxysporum	Ag	5–50	Spherical	Extracellular	[24]

Use of bacteria

Bacteria are among the most extensively exploited natural resources for synthesis of metallic nanoparticles. The key reason for bacterial preference for nanoparticle synthesis is their relative case of manipulation. The figure 1.4.7 probable mechanism for the formation of silver nanoparticles involves the enzyme nitrate reductase [51].

In 2008, silver nanoparticles in the range of 50 nm were synthesized by the supernatant of *B. licheniformis* when silver nitrate was added to it. The synthesized silver nanoparticles were highly stable. Also, the time required for reaction completion was 24 hour. Biosynthesis of silver nanoparticles using microorganisms is

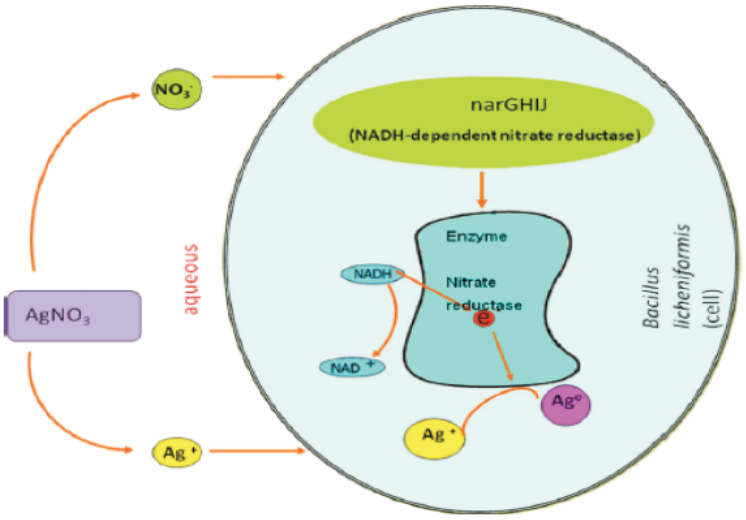

FIGURE 1.4.7: Possible mechanism for silver nanoparticles synthesis in *B. licheniformis* for the biosynthesis of nanoparticle involving NADH-dependent nitrate reductase enzyme that may convert Ag+ to Ag0 through electron shuttle enzymatic metal reduction process

rather slow. However, finding microorganisms to synthesize Ag nanoparticles is an important aspect [51].

Use of fungi

The use of fungi in the synthesis of nanoparticles is a relatively recent adition to the list of potentially revelant microorganism. The use of fungi is potentially exciting since they secrete large amount of enzymes [6]. In most studies, the nanoparticles are formed intracellular, but may be released into solution by suitable treatment of the biomass. Some fungi when challenged with aqueous metal ions lead to the formation of nanoparticles both intra and extracellular [82]. Production of nanoparticles though fungi has several advantages. They include tolerance towards high metal nanoparticle concentration in the medium, easy management in large-scale production of nanoparticles, good dispersion of nanoparticle [64].

Fussarium oxysporum, cationic proteins of around 55kDa in *Veticillum* sp, and glutathione, as well as phytochelatins and metallothioneins in *Saccharomyces cerevisiae*, *Schizosaccharomyces pombe*, and *Candida glabrata*, have been found to be involved in the reduction of metal ions to nanoparticles [29].

Use of plants

Using plants for nanoparticle synthesis can be advantageous overt other biological

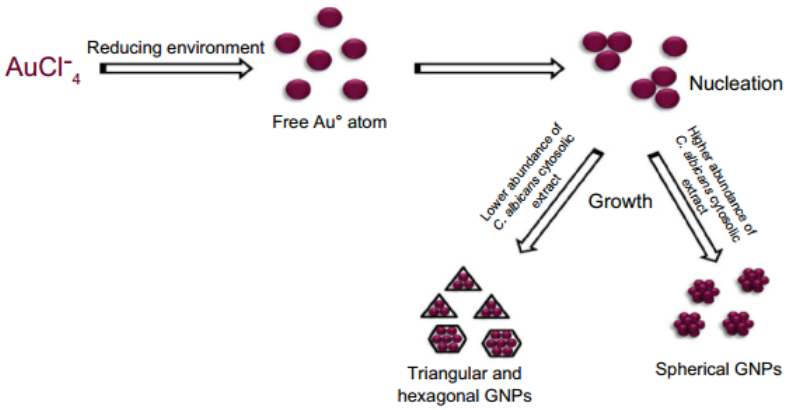

FIGURE 1.4.8: Mechanism of C. albicans cytosol mediated gold nanoparticles

processes because it eliminates the elaborate process of maintaining cell cultures and can also be suitably scaled up for large-scale nanoparticle synthesis [58]. The first report of the plant employed in the synthesis of nanoparticles is attributed to *Medicago sativa* (alfalfa) which was capable of synthesizing gold and silver nanoparticles. The production of nanoparticles by plants relays on various factors among which, type of processing with optimized parameters is very much essential towards synthesis of nanoparticles such as growing plant in a media incorporated with raw material for the synthesis of nanoparticles, use of dried powdered plant material which is employed in the synthesis of plant material, drying plant material and evaluating nanoparticles synthesis, and employing fruits and flowers in the synthesis of nanoparticles [11]. The table 1.4.2 represents some plant species capable of synthesizing nanoparticles.

TABLE 1.4.2: Metal nanoparticles synthesized by plants

Plant	Metal	Size (nm)	Location	Reference
Avena sativa	Au	5-85	Intracellular	[28]
Azadirachta indica	Ag, Au and Ag/Au	50-100	Extracellular	[27]
Aloe vera	Ag	13-19	Not available	[12]
Medicago sativa	Ti/Ni	1-4	Not available	[25]
Emblica Officinalis	Ag and Au	10-20 and 15-25	Extracellular	[9]
Pelargonium graveolens	Ag	16-40	Extracellular	[26]
Cinnamomum camphora	Au and Ag	55-80	Extracellular	[16]
Tamarindus indica	Au	20-40	Extracellular	[10]
Eichhornia crassipes	Mn	1-4	Extracellular	[15]

Eichhornia crassipes

Eichhornia crassipes also known as water hyacinth is a perennial aquatic plant

native of tropical and subtropical regions [**ion**]. Water hyacinth has been established as a pest because is vastly found in lakes, rivers, and other water bodies; it is exploit has been considered useless for several applications because of the high content of tannins [15].

The total heavy metal content of water hyacinths from Valsequillo reservoir located in Puebla, is about 10 089.18 mg/Kg d.w., which indicates that the plant can be considered a hyperaccumulator. On the other hand, the power of bioaccumulation of the water hyacinth represents serious problems for systems, because when the plant is degraded, the reincorporation of metals back into the ecosystem takes place, concentrating in specific parts of the plant. The metals in the plants cause toxicity when they are consumed by other organisms and these in turn can incorporate into the rest of the trofics links. Particularly, the bioaccumulation factors (BF) in the different parts of water hyacinth show that the root (42.54%) has the biggest capacity of bioaccumulation in the plant. In this case it is important to notice that the BF in the water hyacinth for the different elements decreases in the sequence: Mn > Fe > Zn > Cr > Ni ¿ Cu. This means that the water hyacinth has a great affinity to incorporate transition metals; in this case the Mn is accumulated in the biggest concentration in spite of low levels in water (0.44 mg/liter), denoting a high chemical affinity of the biomass to the metal [14].

1.5 Characterization of metal nanoparticles

Dynamic Light Scattering (DLS)

Dynamic Light Scattering is also known as Photon Correlation Spectroscopy. This technique is one of the most popular methods used to determine the size of particles [100]. DLS measures Brownian motion and relates this to the size of the particles. Brownian motion is the random movement of particles due to the bombardment by the solvent molecules that surround them. Normally DLS is concerned with measurement of particles suspended within a liquid [57].

Shining a monochromatic light beam, such as a laser, onto a solution with spherical particles in Brownian motion causes a Doppler Shift when the light hits the moving particle, changing the wavelength of the incoming light. This change is related to the size of the particle [100]. The larger the particle, the slower the Brownian motion will be [57]. It is possible to compute the sphere size distribution and

give a description of the particle's motion in the medium, measuring the diffusion coefficient of the particle and using the autocorrelation function [100].

The size of a particle is calculated from the translational diffusion coefficient by using the Stokes-Einstein equation:

$$d(H) = \frac{kT}{3\pi\eta D}$$

FIGURE 1.5.1: Stokes-Einstein equation

where:
d(H) = hydrodynamic diameter
D = translational diffusion coefficient
k = Boltzmann's constant
T = absolute temperature
n = viscosity

The diameter that is measured in DLS is a value that refers to how a particle diffuses within a fluid. The diameter that is obtained by this technique is the diameter of a sphere that has the same translational diffusion coefficient as the particle. The translational diffusion coefficient will depend not only on the size of the particle "core", but also on any surface structure, as well as the concentration and type of ions in the medium [57]. Also, sample polydispersity can distort the results, and we could not see the real populations of particles because big particles presented in the sample can screen smaller ones [42].

Ultraviolet–Visible Spectroscopy (Uv-Vis)

Ultraviolet- Visible Spectroscopy is a technique used to quantify the light that is absorbed and scattered by a sample (a quantity known as the extinction, which is defined as the sum of absorbed and scattered light). In its simplest form, a sample is placed between a light source and a photodetector, and the intensity of a beam of light is measured before and after passing through the sample. These measurements are compared at each wavelength to quantify the sample's wavelength dependent extinction spectrum. The data is typically plotted as extinction as a

function of wavelength. Each spectrum is background corrected using a "blank" – a cuvette filled with only the dispersing medium – to guarantee that spectral features from the solvent are not included in the sample extinction spectrum [79].

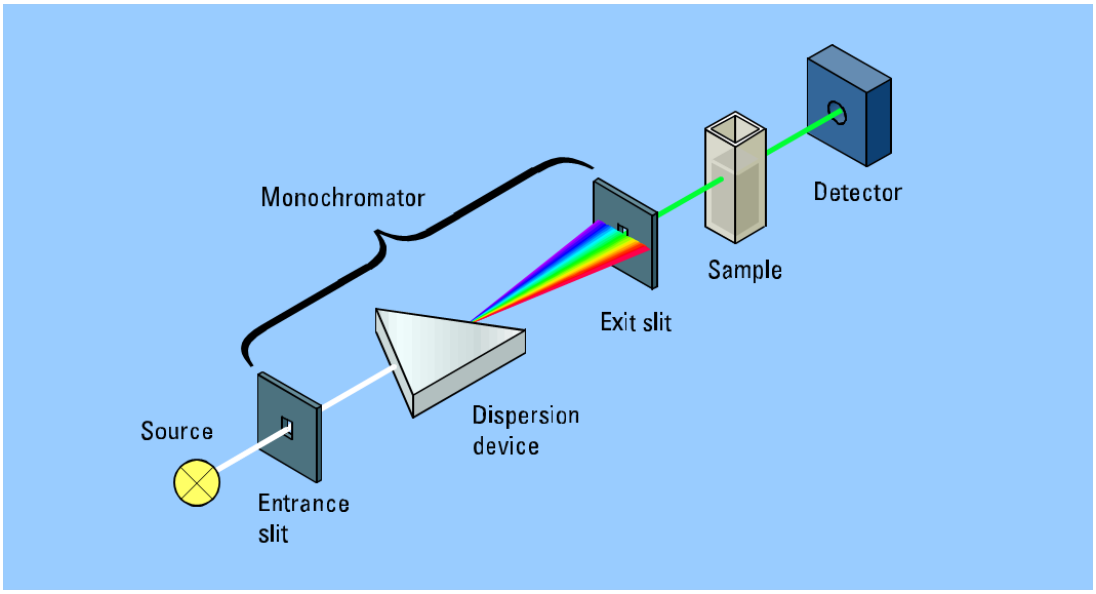

FIGURE 1.5.2: Instrumentation of Ultraviolet–Visible Spectroscopy

UV-Vis spectroscopy can be used as an tool to characterize the properties of metal nanoparticles, in particular the size and shape of the metal nanoparticles and their surface property in the state of the colloidal dispersion system [66], [42], Ag nanoparticles have been investigated actively from the fundamental point of view to understand the mechanism of Ag (I) reduction and Ag nanoparticle formation. This would be because Ag(I) is a simple monovalent metal cation, and the formed Ag clusters have a size-dependent absortion property [66].

Scattering from a sample is typically very sensitive to the aggregation state of the sample, with the scattering contribution increasing as the particles aggregate to a greater extent. For example, the optical properties of silver nanoparticles change when particles aggregate and the conduction electrons near each particle surface become delocalized and are shared amongst neighbouring particles. When this occurs, the surface plasmon resonance (SPR) shifts to lower energies, causing the absorption and scattering peaks to red-shift to longer wavelengths. UV-Visible spectroscopy can be used as a simple and reliable method for monitoring the stability of nanoparticle solutions. As the particles destabilize, the original extinction peak will decrease in intensity (due to the depletion of stable nanoparticles), and

often the peak will broaden or a secondary peak will form at longer wavelengths (due to the formation of aggregates) [79].

Fourier-Transform Infrared Spectrometry

Infrared spectroscopy is associated with vibrational energy of atoms or group of atoms in a material [67]. In infrared spectroscopy, IR radiation is passed through a sample. Some of the infrared radiation is absorbed by the sample and some of it is passed through (transmitted). The resulting spectrum represents the molecular absorption and transmission, creating a molecular fingerprint of the sample. Like a fingerprint no two unique molecular structures produce the same infrared spectrum [81], [67]. Infrared spectroscopy is a nondestructive, highly sensitive technique that provides information about impurities, chemical environment, and free-carrier properties [68].

A method for measuring all of the infrared frequencies simultaneously, was developed which employed a very simple optical device called an interferometer. The Michelson interferometer produces interference fringes by splitting a beam of monochromatic light so that one beam strikes a fixed mirror and the other a movable mirror. When the reflected beams are brought back together, an interference pattern results [109].The interferometer produces a unique type of signal which has all of the infrared frequencies "encoded" into it. The signal can be measured very quickly, usually on the order of one second [81].

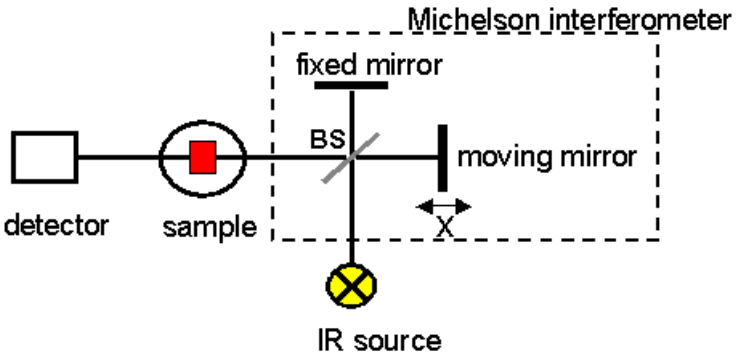

FIGURE 1.5.3: Michelson Interferometer

Fourier transform infrared spectroscopy (FTIR) measurements were carried out to identify the possible biomolecules responsible for reduction, capping of the Ag nanoparticles.

Transmission Electron Microscopy (TEM) and high resolution (HRTEM)
The transmission electron microscope (TEM) operates on the same basic principles as the light microscope but uses electrons instead of light [84].

The general Transmission Electron Microscope (TEM) system. At the top of the TEM is the source of the free electrons. Directly below the source is the condenser system. The condenser system focuses the electrons onto the sample. Below the sample is the objective lens and aperture which collect and convey the electrons to the projector system. The projector system (drawn here as a large lens) usually consists of 2-3 lenses and 1-3 apertures. The imaging surface could be a phosphor screen or the entrance to a CCD camera imaging system [61]. Finally, the chemical analysis system is the energy disperse x-ray spectroscopy (EDS) can be used complimentary to quantify the chemical composition of the specimen [71].

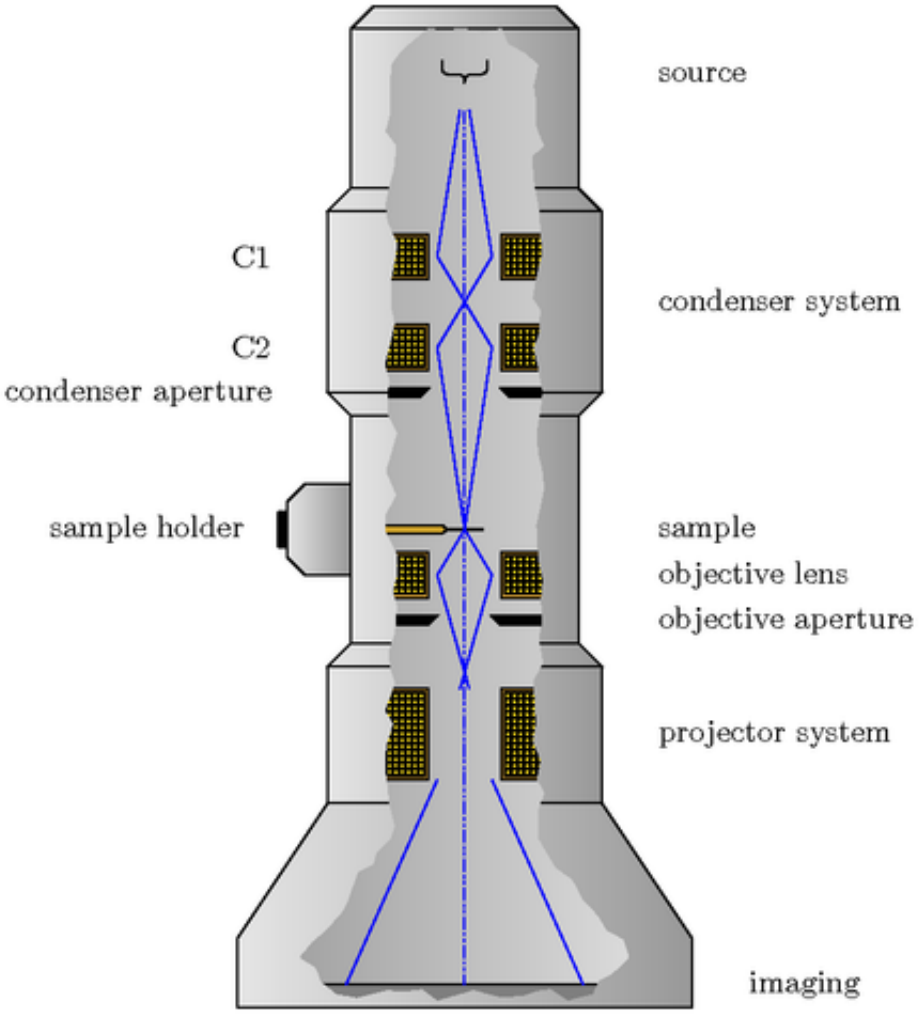

FIGURE 1.5.4: Transmission Electron Microscope System

In TEM, a thin sample, typically less than 200 nm, is bombarded by a highly focused beam of single energy electrons. The beam has enough energy for the electrons to be transmitted through the sample, and the transmitted or scattered electron signal is greatly magnified by a series of electromagnetic lenses. The magnified signal may be observed by electron diffraction, amplitude-contrast imaging such as diffraction contrast, or phase-contrast imaging such as high resolution TEM [69].

Transmission electron microscopy (TEM) as a powerful tool has been extensively used to investigate the morphologies and size distribution of the synthesized Ag-NPs [116].

The measurement of individual unagglomerated spherical particles is straightforward. However, when nanoparticles are bound together or have an irregular shape, accurate size statistics can be more complicated to obtain. Two primary factors influence how a sample is distributed on a TEM grid following preparation, dynamics associated with the drying process and solution concentration. The former process typically leads to a non-uniform distribution of particles on the TEM grid, with some areas of the TEM grid containing few particles and some areas of the grid containing a denser sample [36].

Surface defects and planar defects can be imaged directly using HRTEM [71]. HRTEM can provide structural information at better than 0.2 nm spatial resolution. High magnification imaging requires a high electron dose, so specimens need to be relatively beam insensitive. The technique, by itself, provides very limited chemical information [108].

In this thesis, I worked on a method called *digital darkfield imaging*or simply *DF method* which is used to analyse digitized hihg resolution trnsmission electron microscopy (HRETM) images. The method uses Fourier space filtering to from so called darkfield images in direct space. The brightness and the phase of these complex valued images can be used to analyse periodicities, and changes therein. The selection of frequencies in Fourier space in this digital method is analogous to the selection of a beam of scattered electrons in a TEM [96].

Chapter 2

Materials & Methods

2.1 Materials

This section describes all experimental parameters (chemicals, amounts, materials) used in the experiment. The equipment used for characterization is describe in the appropriate sections.

•*Sampling of the water hyacinth in Valsequillo reservoir*

For the collection of water hyacinth were used plastic containers of 13L and buckets of 19L. Soap were not used for washing the water hyacinth.

•*Processing of biomass*

For the drying of biomass by solar radiation were construct a solar oven (box) with aluminum foil food container and aluminium foil. To pulverize the biomass were used a mortar and a pestle of porcelain and then a laboratory blender (Waring 21-8010EG). The filtering that were made during the washes were carried through a white cotton cloth, and were used a new for each filtration.

•*Synthesis of nanoparticles*

For the synthesis of Ag nanoparticles were used buffer solutions at different pH (4, 5, 7, 9 and 11.33) to determine if the pH in the solution has a impact on the particle formation, Table 2.1.1. Two different concentrations of silver nitrate (AgNO3 from Sigma-Aldrich) are tested Table 2.1.2 to determine if the amount of silver ions in the solution has an impact on particle formation. The ultrasonic bath was through a Crest 275T Tru-Sweep ultrasonic cleaner. Analog model with timer. 3/4 gallon, ID: 9.25 x 5.25 x 4. Centrifugations were through a Thermo Electron Corporation Bench-Top Centrifuge HN-SII.

TABLE 2.1.1: Buffer solution used for synthesizing nanoparticles

pH	Brand	Solution
11.33	HYCEL	Sodium hydroxide glycolate-sodium chloride
5.00	MERCK	Citric acid - sodium hydroxide
4.00	J.T. BAKER	Potassium Biphthalate
9.00	HYCEL	Boric acid- potassium chloride- sodium hydroxide
7.00	MERCK	Potassium dihydrogen phosphate - disodium hydrogen phosphate

TABLE 2.1.2: Concentration of AgNO3 used for AgNP synthesis

Concentration	
1*10-4M	LOW
3*10-4M	HIGH

2.2 Methods

This section describes the procedures used for synthesizing Ag nanoparticles and those for its characterization. The first section describes the procedure of the processing of biomass, the next section describes how the synthesis is carried out, an the last section describes the characterization of the synthesized nanoparticles (Figure 2.2.1).

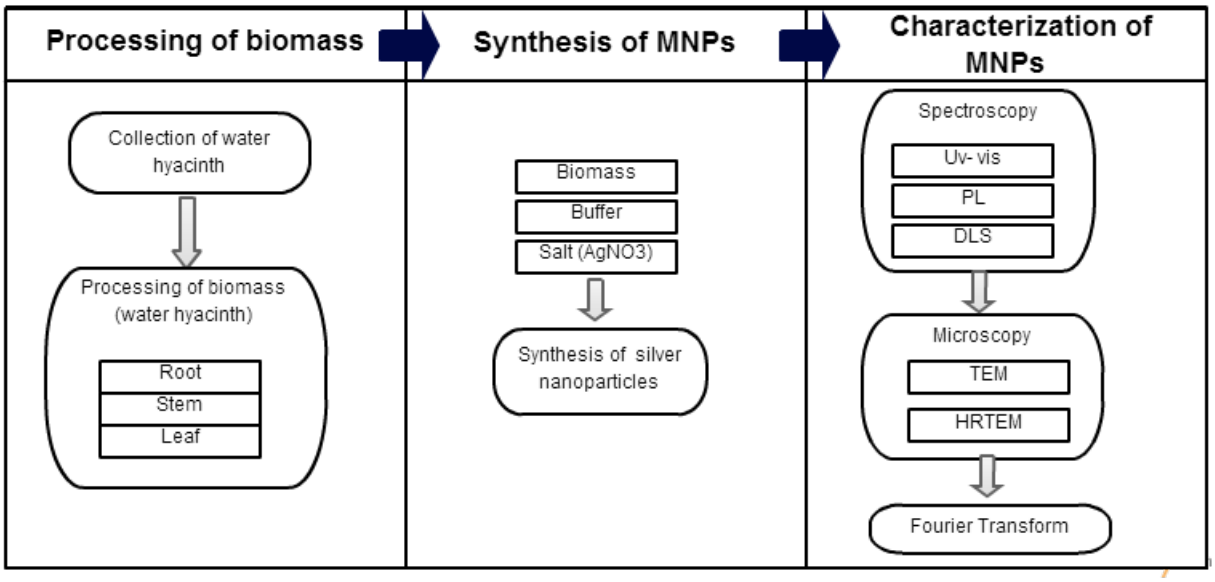

FIGURE 2.2.1: A diagram of methods

Sampling of the water hyacinth in Valsequillo reservoir

It was selected and collected and 1m2 of adult individuals, it placed in plastic containers with water to prevent to die. Immediately it was transported to the

laboratory for processing and washing (Figure 2.2.2) .The taking, transportation and storage of the samples were performed according to the Official Mexican Standard NMX-AA-014-1980.

(A) Valsequillo reservoir (B) 1m2 of individuals (C) Storage

FIGURE 2.2.2: Sequence of the collection of Water hyacinth

Processing of biomass (water hyacinth)

The collected water hyacinth was separated into leaf, root and stem, each part separately were washed with water until clear. Subsequently, water hyacinth was cut into small pieces to facilitate its drying by solar radiation (3 h) . These little pieces of water hyacinth dry, were pulverize with a mortar and pestle and then with a blender which powder was washed with a solution of hydrochloric acid (HCl) at a concentration 0.01N , leaving to stand for 30 min; this wash was performed 2 times. Biomass after filtering (washed with HCl) was placed in aluminum recipients for dehydrating in a preheated oven at 80 C for 24 hours (Figure 2.2.3).

FIGURE 2.2.3: Schematic processing of biomass

Synthesis of nanoparticles

In order to establish the required experimental conditions for obtaining nanoparticles with sizes < 10 nm using the method developed by G. Rosano-Ortega et al, 2006., it was carried out a systematic study of the effects on the synthesis, evaluating variables such as: pH (3, 4, 5, 7, 9 and 11.33), concentration of metal salt (AgNO3), and section of the plant (stem, root, leaf) All the samples and their

synthesis parameters are listed in Table 2.2.1.

TABLE 2.2.1: Parameters of silver nanoparticles synthesis

Sample	[AgNO3]	Section of Plant	pH
R4	LOW/HIGH	root	4
R5	LOW/HIGH	root	5
R7	LOW/HIGH	root	7
R9	LOW/HIGH	root	9
R11	LOW/HIGH	root	11
T4	LOW/HIGH	stem	4
T5	LOW/HIGH	stem	5
T7	LOW/HIGH	stem	7
T9	LOW/HIGH	stem	9
T11	LOW/HIGH	stem	11
H4	LOW/HIGH	leaf	4
H5	LOW/HIGH	leaf	5
H7	LOW/HIGH	leaf	7
H9	LOW/HIGH	leaf	9
H11	LOW/HIGH	leaf	11

The procedure for the synthesis of nanoparticles is a follows (Figure 2.2.4):

1.- A solution with concentration 3x10-4M and 1x10-4 M of the metal salt (AgNO3) was prepared with deionized water.
2.- In a balance was weighed 0.125 g of biomass and was dispensed into polyethylene tubes of 25mL. Subsequently, was added 25mL of deionized water.
3.- The tubes were placed in ultrasonic bath for 15 minutes; 5 min after, the samples were centrifuged for 30 minutes at 3000rpm.
4.- To each sample was added 25 mL of buffer solution (pH = 4, 5, 7, 9 and 11.33).
5.- The samples were exposed to an ultrasonic bath for 15 minutes; 5 min after the samples were centrifuged for 30 minutes at 3000rpm.
6.- To each sample was added 25ml of the metal solution (AgNO3).
7.- The samples were exposed to an ultrasonic bath for 15 minutes; 5 min after the samples were centrifuged for 30 minutes at 3000rpm.
8.- The biomass was separated from the solution by vacuum filtration.

Characterization of Nanoparticles

The synthesized nanoparticles were analyzed by UV-visible spectroscopy, Dynamic

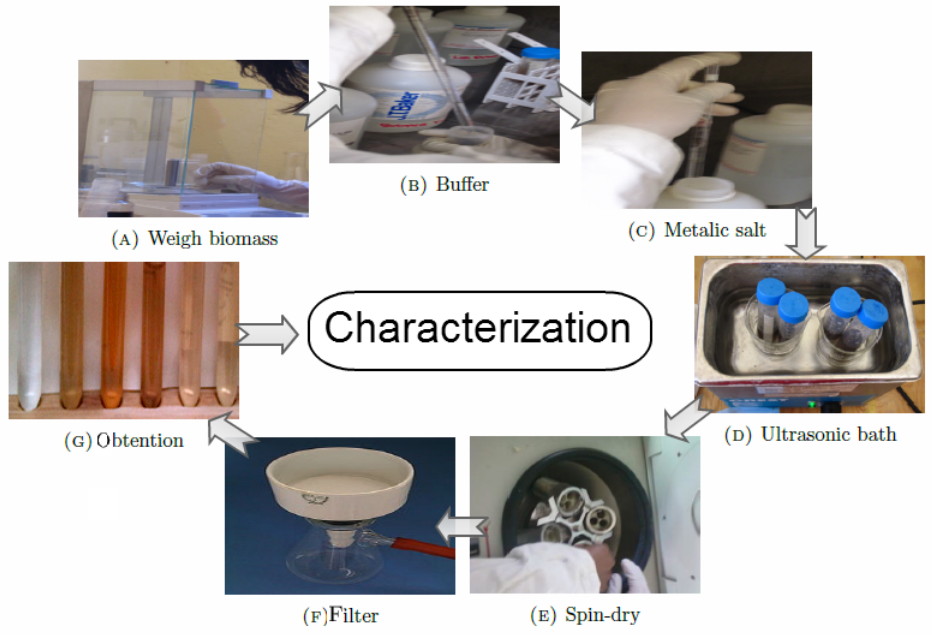

FIGURE 2.2.4: Schematic processing of nanoparticles synthesis

Light Scattering and fluorescence spectroscopy, transmission electron microscopy (TEM) and high resolution (HRTEM). This section describes how the analyses were made.

UV-visible spectroscopy

The optical absorption spectra of AgNP solutions were obtained in a range of wavelength 300-800 nm, using Cary 300 UV-visible spectrophotometer (the blanks used were only distilled water). Analyses were conducted in collaboration with the Center for Nanoscience and Nanotechnology (CNyN) at the UNAM, Ensenada.

TEM & HRTEM

•*Preparation of the sample*

With a Paster pippette a drop of the solution of AgNP was placed on a micro-copper grid covered with carbon type 30-A Pelco brand mesh and allowed to dry at ambient, then proceeded to deposit other droplet. Once prepared the grids, with the aid of an inverse mark magnetically clamp Pelco #4, the samples were taken to the specimen vial to be analyzed by TEM.

•*Analysis of the sample*

Based on the above, the analysis by TEM and HRTEM carried out, using a TEM JEOL JEM-2010F FasTem with 2.3 Å of resolution, at Institute of Physics at UNAM, which has an x-ray detector coupled to perform of energy disperse spectroscopy (EDS). HRTEM images obtained were digitized using a CCD camera Sensys obtaining high resolution images (digital) that were processed using filters in Fourier space. Also, the elemental composition of these aggregates was evaluated using EDS.

Chapter 3

Results

In this chapter the results obtained are presented. The chapter is split into sections describing the results obtained from each measuring method. The results from each method will also be discussed individually in chapter four.

3.1 UV-visible spectroscopy (UV-Vis)

The yellowish-brown color of aqueous silver solution is due to an intense surface plasmon absorption band, which depends on the method of preparation [52]. Absorption in a silver nanoparticle solution can therefore be studied spectrometrically .
The results from absorbance spectroscopy of the samples listed in Table 2.2.1 are presented in this section.

Leaf samples

The figures 3.1.1a and 3.1.1b shows the spectra of samples made with the leaf of water hyacinth at two concentrations 1*10-4M and 3*10-4M of silver nitrate at 4 buffers (pH 5,7,9 and 11).

In the case of samples with low concentration (figure 3.1.1a) , we can see that all samples present a peak located at $\sim$ 280 nm. Sample H15 present a second peak located at $\sim$ 325nm. And sample H111 present a second peak located at $\sim$ 325nm, and a third at $\sim$ 410nm.

The spectra of the samples with high concentration (figure 3.1.1b) are very similar to the samples with low concentration. Because all samples present a peak at ∼ 280 nm . But sample H35 present a second peak at ∼ 325nm, as well as we see in the sample H15. We can also observe that sample H311 present a second peak at ∼ 410 nm, like sample H111.

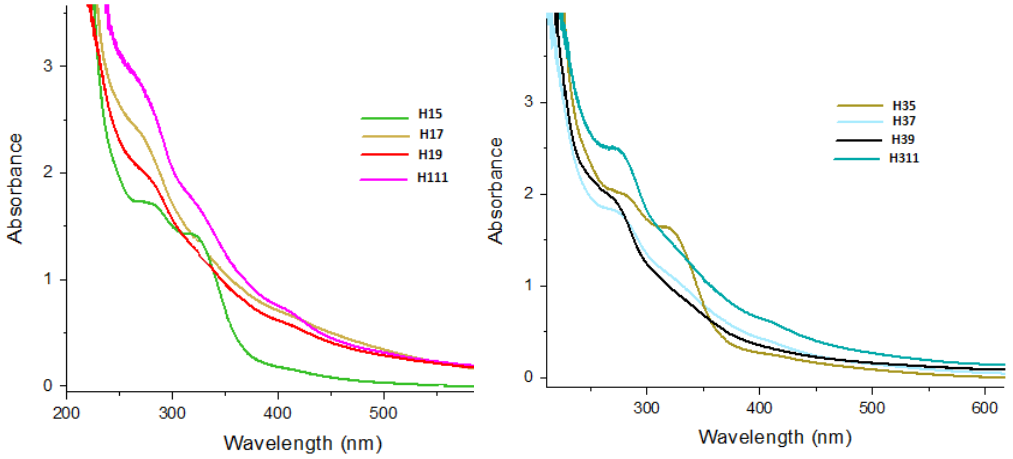

(A) Low concentration (B) High concentration

FIGURE 3.1.1: Absorbance spectra of the solutions made with leaf with two concentrations of silver nitrate

Root samples

The figures 3.1.2a and 3.1.2b shows the spectra of samples made with root of water hyacinth at two concentrations 1*10-4M and 3*10-4M of silver nitrate at 2 buffers (pH 7 and 9).

The spectra for samples with low concentration (figure 3.1.2a), shows that sample R19 present a peak at ∼ 280 nm. Sample R17 present peak at ∼ 300 nm. And sample R111 present a double peak structure the first peak located at ∼280 nm and the second at ∼ 350 nm.

The spectra for samples with high concentration (figure 3.1.2b), shows that sample R37 present a wide peak at ∼ 420 nm. Sample R39 present two peaks, the first at ∼ 280 nm and the second at ∼ 350 nm.

We can see how the peaks are very similar to the peaks of the samples of leaf.

Stem samples

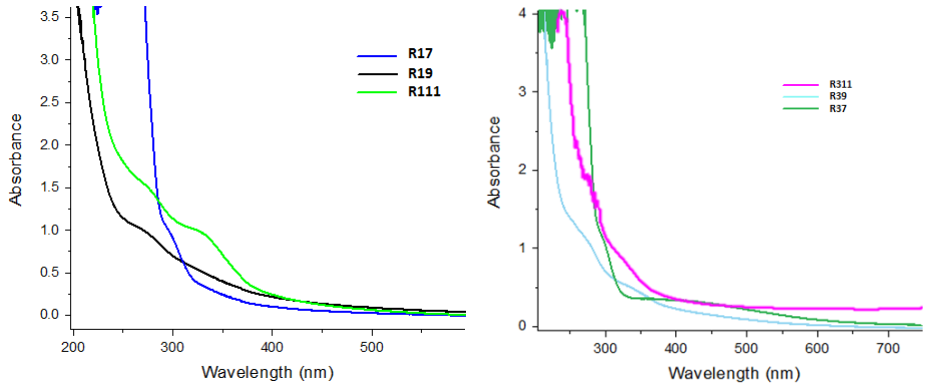

(A) Low concentration (B) High concentration

FIGURE 3.1.2: Absorbance spectra of the solutions made with root with two concentrations of silver nitrate

The figures 3.1.3a and 3.1.3a shows the spectra of samples made with stem of water hyacinth at two concentrations 1*10-4M and 3*10-4M of silver nitrate at 4 buffers (4,7 9 and 11).

The figure 3.1.3a show that the sample T111 present three peaks, the fist at ∼ 280 nm, the second at ∼325 nm and the third at ∼410 nm. Sample T14 present a peak at ∼ 320 nm and finally sample T17 present a peak at ∼ 310 nm.

In the figure 3.1.3b we can see that all samples T311, T37, T39 and T34 , present a peak at ∼ 410nm. The sample T311 also show a peak at ∼280 nm.

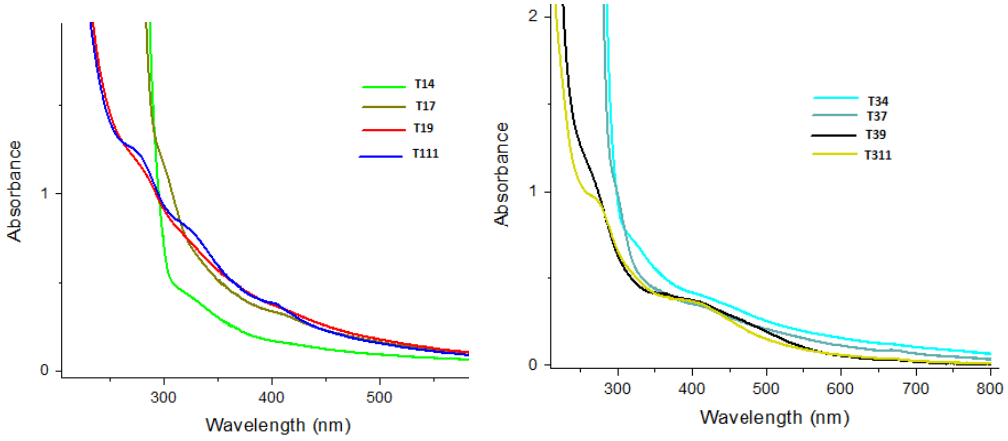

(A) Low concentration (B) High concentration

FIGURE 3.1.3: Absorbance spectra of the solutions made with stem with two concentrations of silver nitrate

The table 3.1.1 shows the Absorbance peaks of all samples

TABLE 3.1.1: The peaks of the samples

Sample	Peak (nm)	Sample	Peak (nm)
R17	300	R37	420
R19	280	R39	280/350
R111	280/350	R311	–
T14	320	T34	410
T17	310	T37	410
T19	–	T39	410
T111	280/325/410	T311	410/280
H15	280/325	H35	280/325
H17	280	H37	280
H19	280	H39	280
H111	280/325/410	H311	280/410

To know the effect and interaction of the three variables of study (pH, AgNO3 concentration and plant section), because UV-Vis absorption results, it was constructed and analysis of variance (ANOVA), with a significance level of 5%. In this analysis the plant section was considering as a block.

Source	DF	Seq SS	Adj SS	Adj MS	F	P
ph	3	1.0000	1.0000	0.3333	1.60	0.229
conc metal	1	0.6667	0.6667	0.6667	3.20	0.093
ph*conc metal	3	0.3333	0.3333	0.1111	0.53	0.666
Error	16	3.3333	3.3333	0.2083		
Total	23	5.3333				

FIGURE 3.1.4: Analysis of variance of UV-Vis absortion results

To interpret the data, we take into account the P-value and the the significance level. If the P-value is lower than the significance level (0.05) the variable has an effect on the result; if it is higher, the variable has not an effect. According to this results, the concentration of AgNO3 has an effect on the production of silver nanoparticles and pH has not an effect according to the ANOVA.

3.2 Dynamic light scattering (DLS)

Particle size can be determined by measuring the random changes in the intensity of light scattered from a suspension or solution. DLS is most commonly used to analyze nanoparticles [53]. This section describe the results obtained of randomly selected Ag NP samples (R37, R311, H35, H39,T37).

Root samples

From the figure 3.2.1 it can be seen the particle size distribution obtained of sample *R37*.

•The distribution extends from ∼ 102.2 nm to as much as ∼ 687 nm.

•As table shows that particles below ∼ 10 nm was not detected.

•The central position or P50 of nanparticles have ∼ 344 nm of diameter.

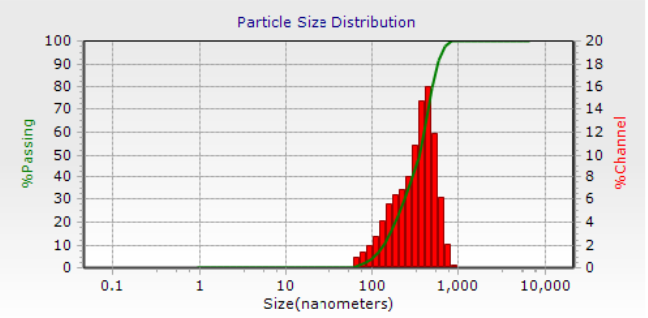

%Tile	Size (nm)
95	687
90	570
80	486
60	392
50	344
40	289
30	243
20	171.9
10	121.5
5	102.2

FIGURE 3.2.1: Particle size distribution of sample R37

From the figure 3.2.2 it can be seen the particle size distribution obtained of sample *R311*.

•The distribution extends from ∼ 17.81 nm to as much as ∼ 586 nm.

•As table shows that particles below ∼ 10 nm was not detected.

•The central position or P50 of nanoparticles have ∼ 36.2 nm of diameter.

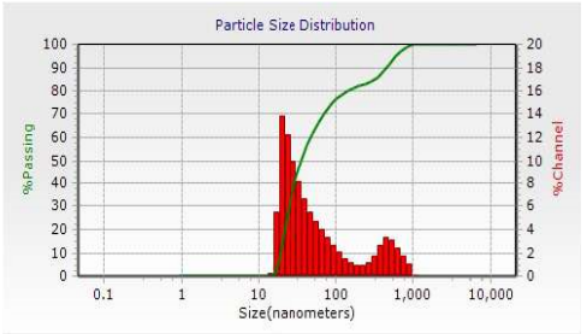

%Tile	Size (nm)
95	586
90	445
80	144.7
60	48
50	36.2
40	29.4
30	24.86
20	21.6
10	19.18
5	17.81

FIGURE 3.2.2: Particle size distribution of sample R311

Leaf samples

From the figure 3.2.3 it can be seen the particle size distribution obtained of sample *H35*.

•The distribution extends from ∼ 7.2 nm to as much as ∼ 39.7nm.

•As the table shows 40% of total are particles below ∼ 9.79 nm.

•The central position or P50 of nanoparticles have ∼ 10.68 nm of diameter.

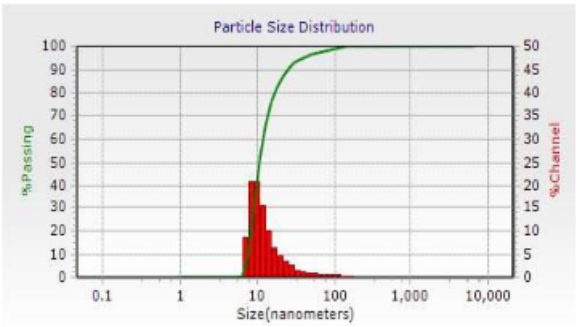

%Tile	Size (nm)
95	39.7
90	24.95
80	16.88
60	11.84
50	10.68
40	9.79
30	9.07
20	8.3
10	7.69
5	7.2

FIGURE 3.2.3: Particle size distribution of sample H35

From the figure 3.2.4 it can be seen the particle size distribution obtained of sample *H39*.

•The distribution extends from ∼ 8.04 nm to as much as ∼ 101.2 nm.

•As table shows 20% of total are particles below ∼ 8.69 nm.

•The central position or P50 of the nanoparticles have ∼ 19.47 nm of diameter.

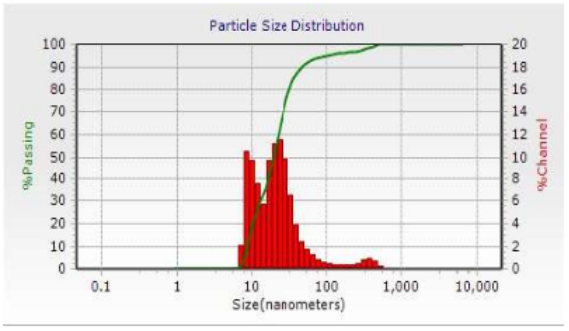

%Tile	Size (nm)
95	101.2
90	48.4
80	31.9
60	22.64
50	19.47
40	16.57
30	12.85
20	10.28
10	8.69
5	8.04

FIGURE 3.2.4: Particle size distribution of sample H39

Stem samples

From the figure 3.2.5 it can be seen the particle size distribution obtained of sample *T37*.

•The distribution extends from ∼ 72.3 nm to as much as ∼ 2750 nm.

•As table shows that particles below ∼ 10 nm was not detected.

•The central position or P50 have ∼ 1156 nm of diameter.

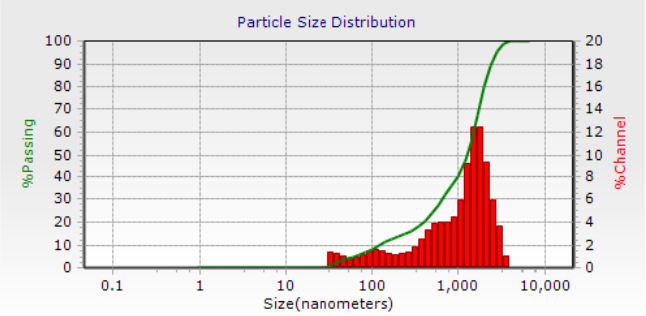

%Tile	Size (nm)
95	2750
90	2312
80	1944
60	1375
50	1156
40	972
30	687
20	409
10	121.5
5	72.3

FIGURE 3.2.5: Particle size distribution of sample T37

3.3 Transmission electron microscopy(TEM) & High resolution (HRTEM)

Through transmission electron microscopy (TEM), images of Ag NP samples selected were obtained, which were analyzed in order to determine the average size to compare to DLS and to obtain the lattice parameters to know its structure, shape and composition.

The sampling in each sample is different, because two reasons *1.*-the nanoparticles per micrograph were few and *2.*- the number of micrograph were few per sample.

Size distribution of AgNP

Root samples

The size distribution of sample *R37*, is shown in figure 3.3.1, considering a samplig of **752** nanoparticles, its was obtained a mean of **5.299** nm and a standard deviation of **2.673** nm.

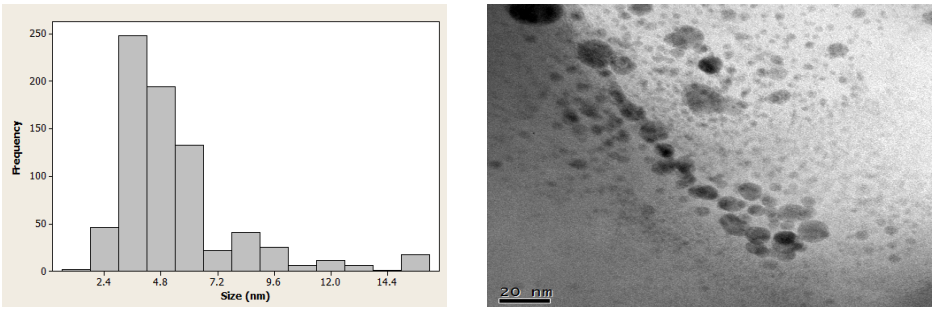

(A) Histogram of size distribution (B) TEM micrograph

FIGURE 3.3.1: Particle size distribution of sample R37

The size distribution of sample *R311* is shown in figure 3.3.2, considering a sampling of **300** nanoparticles, it was obtained a mean of **2.345** nm and a standard deviation of **0.8201 nm**.

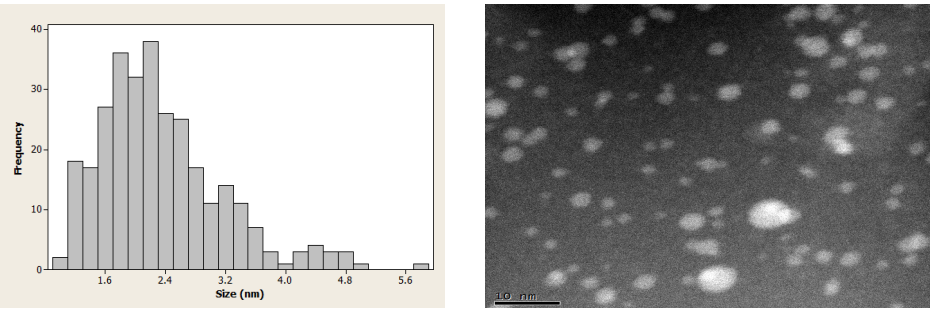

(A) Histogram of size distribution (B) TEM micrograph

FIGURE 3.3.2: Particle size distribution of sample R311

Leaf samples

The size distribution of sample *H35* is shown in figure 3.3.3, considering a sampling of **87** nanoparticles, it was obtained a mean of **9.306** nm and a standard deviation of **7.101** nm.

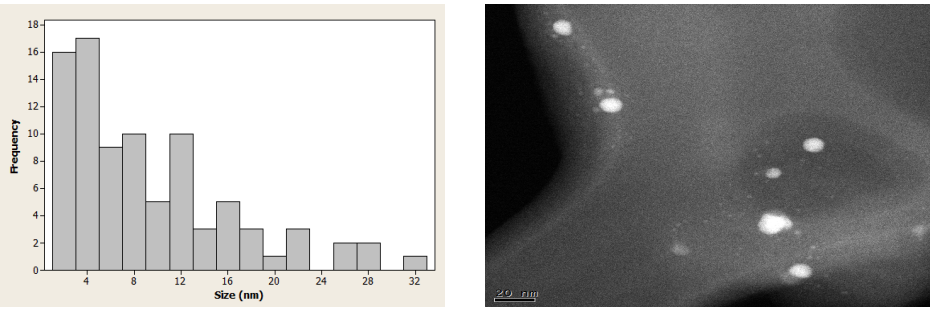

(A) Histogram of size distribution (B) TEM micrograph

FIGURE 3.3.3: Particl size distribution of sample H35

The size distribution of sample *H39* is shown in figure 3.3.4, considering a sampling of **47** nanoparticles, it was obtained a mean of **24.85** nm and a standard deviation of **16.52** nm.

Stem samples

The size distribution of sample *T37* is shown in figure 3.3.5, considering a sampling of **116** nanoparticles, it was obtained a mean of **3.091** nm and a standard deviation of **1.733** nm.

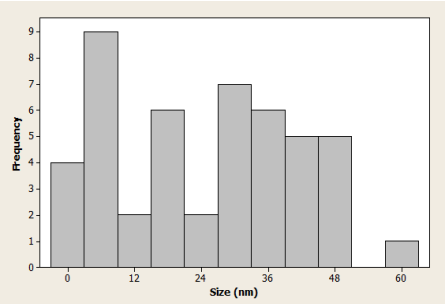

(A) Histogram of size distribution

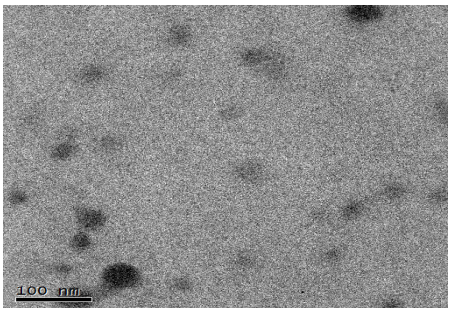

(B) TEM micrograph

FIGURE 3.3.4: Particle size distribution of sample H39

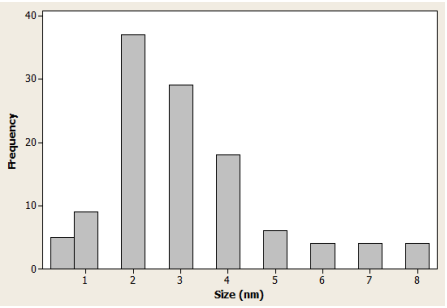

(A) Histogram of size distribution

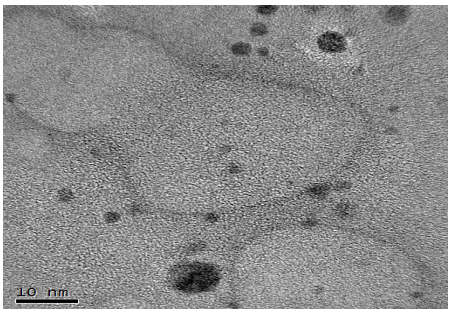

(B) TEM micrograph

FIGURE 3.3.5: Particle size distribution of sample T37

The table 3.3.1 compare the distribution size of the Ag NP obtain by DLS and TEM.

TABLE 3.3.1: Size distribution of Ag NP

Sample	P50	Mean	Distribution
R37	344	5.299	Skewed to the left
R311	36.2	2.345	Skewed to the left
H35	10.68	9.306	Skewed to the left
H39	19.77	24.85	Skewed to the right
T37	1156	3.091	Skewed to the left

Structure of AgNP

The Fourier Transform analysis was used to obtain inter-planar spacings, which determine the Ag phase.

Root samples

The figure 3.3.6 shows the inter-planar spacings obtained in sample *R37* by HRTEM micrographs. According to the tables for crystallography, two different structures

were found, corresponding to two different Ag phases.

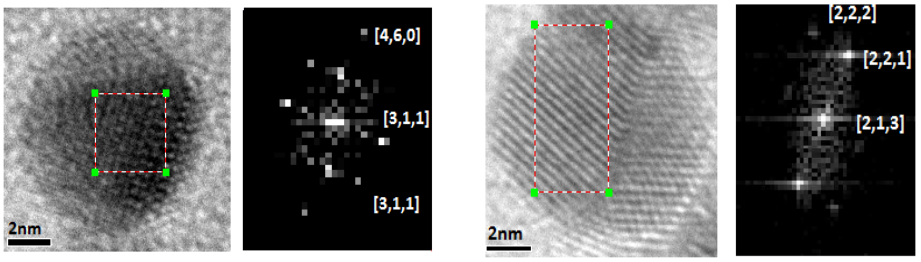

(A) Structure of Ag2O3 (B) Structure of AgO

FIGURE 3.3.6: FFT patrons of HRTEM images in sample *R37*

The figure 3.3.7 shows the inter-planar spacings obtained in sample *R311* by HRTEM micrographs. According of tables for crystallography, it was found only a Ag phase.

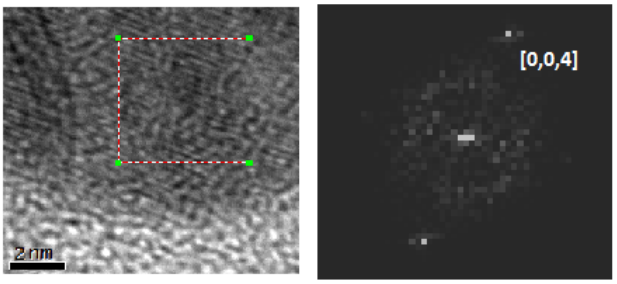

FIGURE 3.3.7: Structure of AgO. FFT patrons of HRTEM images in sample *R311*

Leaf samples

The figure 3.3.8 shows the inter-planar spacings obtained in sample *H35* by HRTEM micrographs. According of tables for crystallography, three different structures were found, corresponding to three different Ag phases.

The figure 3.3.9 shows the inter-planar spacings obtained in sample *H39* by HRTEM micrographs. According of tables for crystallography, two different structures were found, corresponding to two different Ag phases.

Stem samples

The figure 3.3.10 shows the inter-planar spacings obtained in sample *T37* by

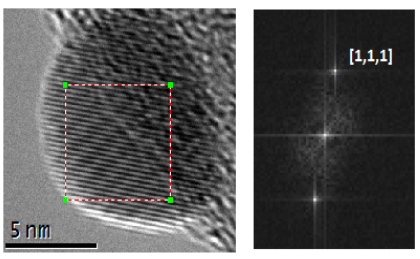

(A) Structure of Ag2O3

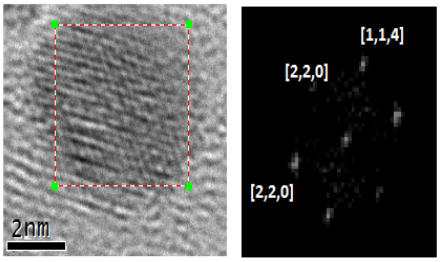

(B) Structure of Ag

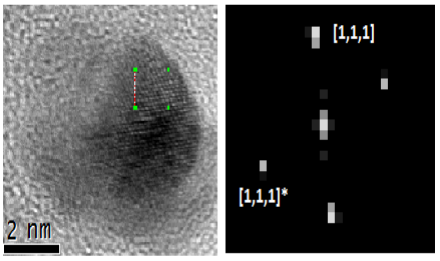

(C) Structure of AgO

FIGURE 3.3.8: FFT patrons of HRTEM images in sample *H35*

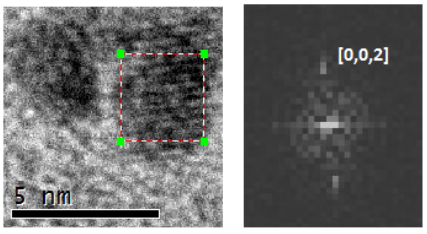

(A) Structure of Ag

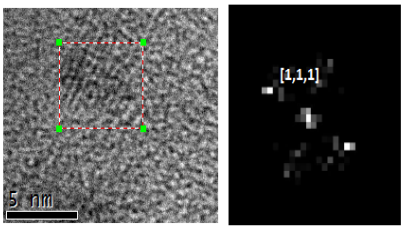

(B) Structure of Ag2O3

FIGURE 3.3.9: FFT patrons of HRTEM images in sample *H39*

HRTEM micrographs. According of tables for crystallography, two different structures were found, corresponding to two different Ag phases.

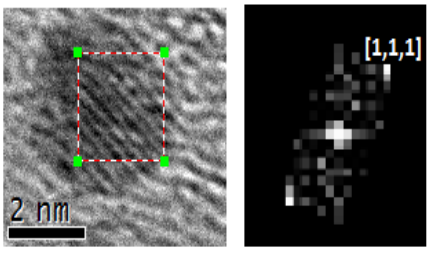

(A) Structure of Ag

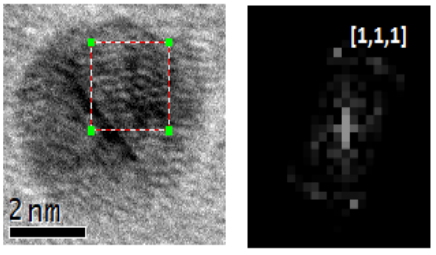

(B) Structure of AgO

FIGURE 3.3.10: FFT patrons of HRTEM images in sample *T37*

The table 3.3.2 shows the corresponding lattice parameters of the samples analyzed by HRTEM.

TABLE 3.3.2: Lattice parameters of silver nanoparticles

Sample	Structure
R37	Ag2O3/AgO
R311	AgO
T37	Ag /AgO
H35	Ag2O3 / Ag /AgO
H39	Ag /Ag2O3

The following table summarizes 3.3.3 the results of the absorbance of Uv-Vis, the size distribution by DLS, and TEM, and the structures obtained by the Fourier Transform. This table includes the number of nanoparticles per area, specifically in $4*10^{-5}$ cm^2.

TABLE 3.3.3: Summary of results

Sample	Absorbance	P50	Mean	Structure	Distribution	#Particles/Area
R37	420	344	5.29	Ag_2 O_3/AgO	Skewed	$219/4*10^{-5}$ cm^2
R311	–	36.2	2.345	AgO	Skewed	$127/4*10^{-5}$ cm^2
T37	410	1156	3.091	Ag /AgO	Skewed	$41/4*10^{-5}$ cm^2
H35	280/325	10.68	9.306	Ag_2O_3/Ag/AgO	Skewed	$22/4*10^{-5}$ cm^2
H39	280	19.77	24.85	Ag /Ag_2O_3	Skewed	$4/4*10^{-5}$ cm^2

Elemental Chemical Composition

Energy dispersive X-ray spectroscopy (EDS) was used to confirm that samples contained elemental silver. We can notice that in all analysis there is present the silver and copper because copper grids were used to support the drop, for TEM analysis. In sample R37 there is also present elements like C, O, P, S, Cl, Ca, Zn, Si, K and Th; probably of the extracts of the plant.

3.4 Fourier transform infrared spectroscopy (FTIR)

FTIR measurements were carried out to identify the possible biomolecules responsible for capping and efficient stabilization of silver nanoparticles 3.4.1. The intense broad absorbance at 3332 cm^{-1} is the characteristic of the hydroxyl functional group in alcohols and phenolic compounds(tannins). The band at 1637 cm^{-1} can be assigned to the amide I band of the poteins releases by water hyacinth, or to C=C groups/aromatic rings [58]. The band at 1321 cm^{-1} are characteristic of the C–O and C=O stretching modes of the carboxylic acid group [87]. The band

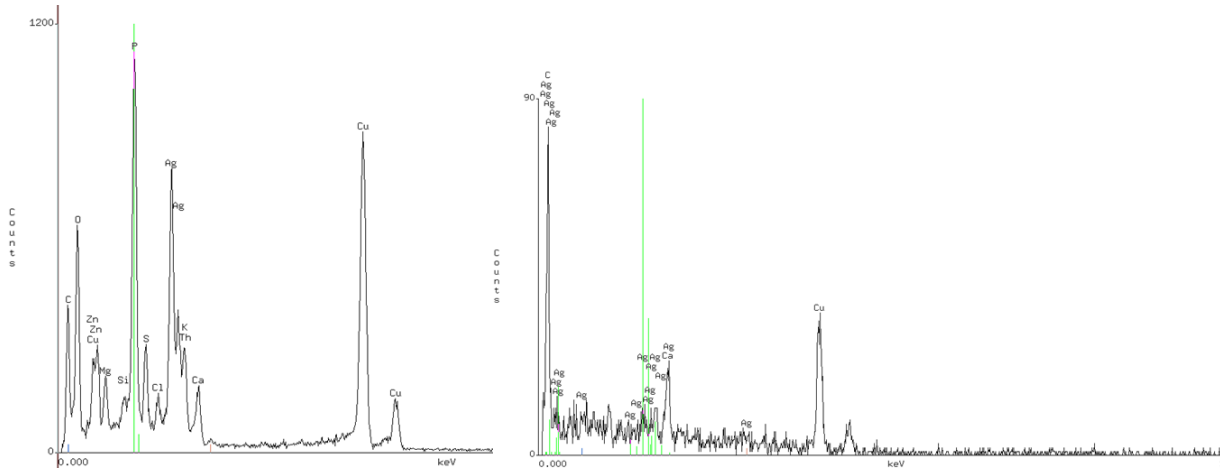

(A) EDS analysis of sample R37 (B) EDS analysis of sample H37

FIGURE 3.3.11: Energy dispersive X-ray spectroscopy analysis

at from 2260-2100 cm^{-1} can be assigned to –C≡C– [75].

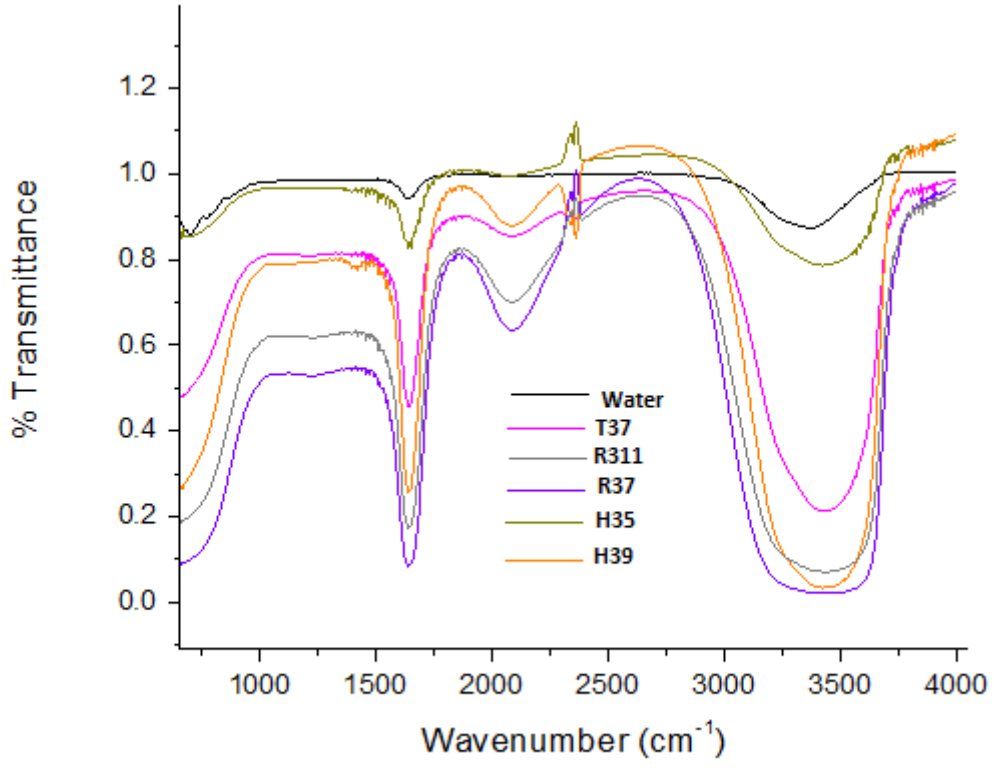

FIGURE 3.4.1: FTIR of silver nanoparticles

Chapter 4

Discussion

In this chapter the results obtained are discussed.

Measuring methods are by their nature difficult to evaluate with respect to their validity. Especially the size and shape of the silver nanoparticles are important matters in this thesis, therefore, it is important to be aware of the possible measuring problems.

4.1 UV-visible spectroscopy

The absorbance spectroscopy is a fast way to obtain data of silver nanoparticle solution. However, these data alone does not tell much about the silver nanoparticles. The color of the silver nanoparticle solutions is due to the excitation of surface plasmon vibrations (essentially the vibration of the group conduction electrons) [64], absorption between 400 – 450 nm is usually characteristic of this [65].

As can be seen in Table 3.1.1, only samples H111, H311, T111, T311, T37, T39, T34, y R37 showed peaks around 410 nm -420 nm as expected from the plasmon resonance of silver nanoparticles. Note that in most of the spectra showed a peak in 280nm, and around 325 nm. This peaks could appeared because of the plant extracts, because chromatographic and spectroscopic analyses showed that macrophytes can release fatty acids, steroids,polyphenols and tannins [99]. Polyphenols displayed a peak visible around 278 nm [43]. We discard that are

Ag+ ions, because the UV-Vis spectra of the AgNO3 solution, has a peak around 217 nm [43].

Other possibility is the obtention of anisotropic particles, because according to Mie's theory, only a single SPR band is expected in the absorption spectra of spherical nanoparticles, whereas anisotropic particles could give rise to two or more SPR bands depending on the shape of the particles. Also, the position and shape of plasmon absorption of silver nanoclusters are strongly dependent on the particle size, dielectric medium, and surface-adsorbed species [107].

4.2 Comparison between DLS and TEM

The Table 3.3.1, compare the size distribution of Ag NP between the median or P50 obtain by DLS and the mean obtain by TEM. According to these results, we can see that samples R37, R311 H35 and T37 are skewed to the left, and H39 skewed to the right.
Comparing the results with the histograms obtained by DLS analysis, the distribution of sample R311 is more bimodal and skewed to the right, and sample H35 is more skewed to the right than to the left.
If we know compare the results with the histograms obtained by TEM analysis, samples R37, R311 H35 and T37 are skewed to the right instead of to the left. And H39 have more a normal distribution.

The most probable cause is because size is not only connected with the metallic core of the nanoparticles but it is also influenced with all substances adsorbed on the surface of the nanoparticles (e.g., stabilizers) [42]. As a consequence, the size measured in DLS technique is bigger in comparison with microscopic techniques as we can observe in the Table 3.3.1. So, we do not measure the size by number as we get by TEM. The number based is only derived mathematically and give us an idea about an average by numbers. However, also means that error is much larger for the smaller particles.

4.3 Structure

As can be seen in Table 3.3.2, the lattice parameters of the samples, correspond to Ag, AgO and Ag_2O_3. So, this result can justify why the peaks in UV-Vis spectroscopy are shifted, and also DLS and TEM particle size distribution analysis shows asymmetric distributions, at the same time in some samples there are large nanoparticles, that may correspond to silver oxide AgO or Ag_2O_3. Because there are different structures in the same sample, its very difficult to know the proportions of each structures, although in sample R311 were found only a structure. In EDS analysis were found silver and others elements that could form of the layer of biomass that protect the nanoparticles. Another possibility is that are part of the extract of the plant that stay in the solution.

4.4 Effect of pH

The pH ranging from acid to basic was studied, but it is difficult to observe a tendency. An analysis of variance (ANOVA) were constructed to determine if the pH has an effect in the formation of silver nanoparticles. As we can see in figure 3.1.4, the pH has no influence in the formation of silver nanoparticles.

In contrast to results by TEM analysis, the pH has a significant influence because samples with the same metal concentration and plant section has different particle size distribution and different Ag phases.

4.5 Effect of AgNO3 concentration

The production of nanoparticles is also dependent on substrate concentration. The concentration of $AgNO^3$ from $1*10^{-4}$M and $3*10^{-4}$M was studied. The concentration which obtained most absorbance peaks typical of Ag nanoparticles was $3*10^{-4}$M; analyzed by UV-visible absorption spectroscopy.This results was corroborated with an ANOVA analysis, show in figure 3.1.4.

4.6 Effect of the plant section

The three sections of water hyacinth obtained peaks around 410 nm. But it is clear, that stem has more typical absorbance peaks for Ag nanoparticles than root and leaf. If we complemented with the results by TEM , we can add that samples with root has more nanoparticles per area; the nanoparticles in samples with leaf are found slightly larger than in root and stem.

4.7 Scale up

The table summarizes 3.3.3 the results of the absorbance of Uv-Vis, the size distribution by DLS, and TEM, and the structures obtained by the Fourier Transform. This table also includes the number of nanoparticles per area, specifically in $4*10^{-5}$ cm^2. Considering that that the main purpose to synthesize silver nanoparticles is to obtain a sustainable method to scale up because of its application as bactericide, we are going to compare all the results to find the best conditions of synthesis.

In the case of the absorbance peak, we can see that root and stem samples have the SPR typical of Ag. Also, this samples, have the lower size. But if we compare the lattice parameters obtained, we can see that only T37 and H39 have Ag in its basal state; also in this samples were obtained AgO and Ag_2 O_3 respectively. If we observe the size distribution obtained by the comparison between P50 by DLS and mean by TEM, the graphs of all samples are skewed, but if we take into account the micrographs, R311 have the most homogenous nanoparticles and it is one of the samples with more nanoparticles per area.

We are also going to define the best condition of synthesis, taking into consideration that bactericidal properties of the nanoparticles are size dependent (diameter of $\sim$ 1–10 nm), having a direct interaction with the bacteria [62]; truncated triangular silver nanoparticles with a 1,1,1 lattice plane as the basal plane display the strongest biocidal action, compared to spherical and rod-shaped nanoparticles and with silver ions [98], [62]; and a large contact surface is expected to enhance

the extent of bacterial elimination [62].

T37 is the best option because:

- Present a peak absorbance at 410 nm, typical for SPR of Ag nanoparticles.
- According to the distribution size by TEM, has a mean of 3.091 nm.
- The graph obtained by the comparison between DLS and TEM show that is skewed to the left, showing that 50% of nanoparticles have a size $\leq$ 3.091 nm (mean).
- Although it was found the lattice parameters correspond to two different Ag phases, the lattice found are [1,1,1], showing potential biocidal properties.
- The number of particles per analyzed area ($4*10^{-5}$ cm^2) in average is of 41 nanoparticles.
- Considering that this method will scale up, it is more easy the washing and dry of stem than root, and also the biomass obtain is more.
- The pH is another advantage because it is neutral, therefore has more chance for biological applications.

4.8 Fourier transform infrared spectroscopy (FT-IR)

The results of the FTIR spectra 3.4.1 indicates that silver nanoparticles synthesized using the water hyacinth are surrounded by some proteins and metabolites such as tannins, terpenoids having functional groups of amines, alcohols, ketones, aldehydes, and carboxylic acids [58]; as chromatographic and spectroscopic analyses showed that macrophytes can release fatty acids, steroids, polyphenols and tannins [99]

So, we can think in possibles mechanism of reduction of silver nanoparticles by water hyacinth.

A possibility is by sugars, because investigations of gold and silver nanoparticles formation within the tissues of Brassica juncea found that the sites of the most abundant reduction of metal salts to nanoparticles were the chloroplasts in which high reducing sugars (glucose and fructose) are responsible for biofabrication of silver and gold nanoparticles [32].

Other possibility is polyphenolic compounds in the plant extracts known as potential reductors agents in the synthesis mechanism of silver nanoparticles. The main mechanism is hydrogen abstraction due to the OH groups in the polyphenol molecules [43].

Also, it is known in plants that when the metals are absorbed by the roots, these must be accumulated in vacuoles, principally in nanoparticle form with just a few atoms, which are reduced by means of defense systems like phytochelatins and other enzymes that are a part of the vacuoles [49].

Chapter 5

Conclusion

In this thesis the biosynthesis of Ag nanoparticles using water hyacinth (*Eichnornia crassipes*) was made. The influence of pH, AgNO3 concentration and part section (root, stem, leaf) was evaluated in their size and structure .

Comparing the size distribution between TEM and DLS we conclude that the last is a mathematical approximation that gives us and idea of the particle size, consequently has more percentage of error.

Three different Ag phases (Ag, AgO and Ag2O3) were found in the samples. It is not possible to know the percentage of these in each sample.

Uv-Vis analysis show that pH has not an effect on the formation of nanoparticles, but TEM analysis says the opposite. The concentration which show an effect on the formation of nanoparticles is 3*10-4M. The section of water hyacinth that show an effect in the particle formation is stem.

The sample that show the best characteristics as bactericide is R37, because present the SPR typical of Ag NP; the size of nanoparticles are lower than 10 nm; the number of nanoparticles per are is moderate, but help to prevent their agglomeration; nanoparticles are homogeneous; although there were found two Ag phases, the lattice parameter found in both is (1,1,1); the pH of the sample it

neutral and the biomass in comparison of root is higher.

This thesis proposed an ecofriendly method for silver nanoparticle synthesis using water hyacinth that is ease with the process and can be scaled up and which nanoparticles can be applied in industry as bactericide.

Chapter 6

Perspectives

This project is the base to research: a) the effect of silver nanoparticles in a variety of microorganism, and the mechanism of antibacterial activity; b) toxicological test because silver nanoparticle could be released from manufactured nanomaterials and enter in aquatic ecosystems c) further testing in the imaging of diseases, such as cancer; d) the scale-up of the method.

Appendix A

Appendix

Distribution of size

In order to calculate the size of synthesized nanoparticles, it was used a software called Digital Micrograph (the image is formed in the microscope and digitized by the CCD camera. The data is then sent to the camera Controller where it is converted to a form that the computer can read. The DMA (direct memory access) card transfers the data from the Controller into the computer's memory where DigitalMicrograph can access the data [48].

The procedure is as follows:

1.-Select the image you want to open from FILE menu. Select from the WINDOWS menu Standard Tools and then the Line Profile tool. 2.-To do a measure, make a line along the diameter of the figure.

3.- A graph appear after making the measure. To recognize the distance of the figure, it is necessary to position the cursor on one of the peaks of the graph and drag to the peak that has the same distance (to adjust the endpoints of a line profile, you can adjust the endpoints of a line profile by two methods.

• Adjust the endpoints by dragging the handles on the line profile.

• Adjust the endpoints by double-clicking on the line profile.

The CHANGE PROFILE INFO dialog will appear. Enter the desired coordinates in this dialog. The coordinates should be specified in uncalibrated units (i.e. pixels)).

Fourier Transform

To calculate the average inter-planar spacings of nanoparticles, a Fourier Transform is done with the same software (Digital Micrograph). The procedure is as

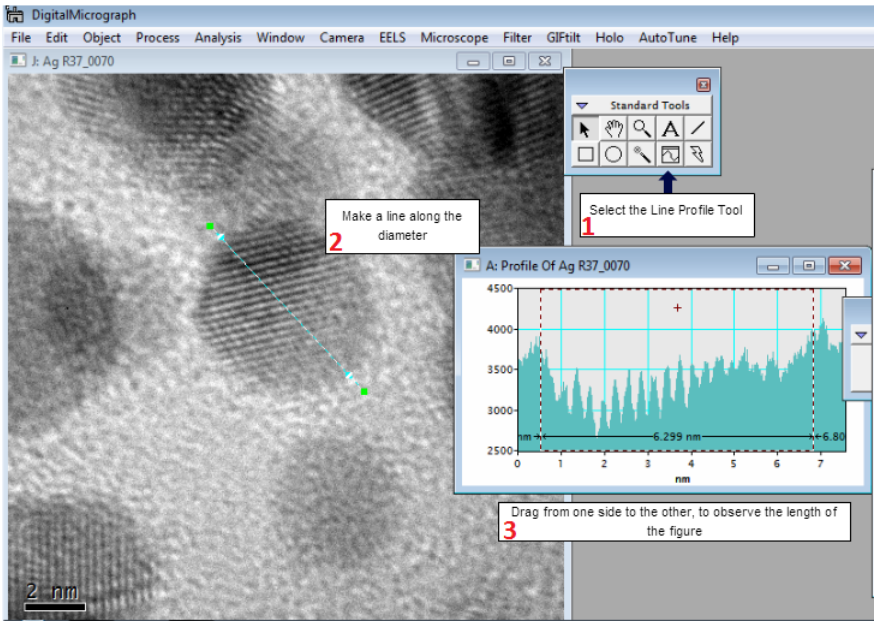

FIGURE A.0.1: Procedure to measure diameters of nanoparticles

follows:

1.- Select the image you want to open from FILE menu. Select with the square from ROI Tools the area of the micrograph yo have to analyze.You can also create a region of interest on the source image with appropriate dimensions by holding down the CTRL + ALT key under Windows while drawing the rectangular region of interest. 2.- Select FFT (CTRL + F) from the Process menu. A new window is now open,and the FFT of the figure is now generated. 3.- To obtain a better display of the image, you can modify the brightness, contrast or gamma with the display control.

4.- To measure the inter-planar spacings, select from the Standard Tools the Line Profile Tool and drag the cursor from one point to the opposite and then adjust the endpoints.

To calculate the inter-planar angles , we used the software MB-Ruler. The procedure is as follows:

1.- Open an image with inter-planar spacing drawn, also opens the Triangular Ruler Tool of MB-Ruler.

2.- Put the center of the Triangular Ruler above the center of the image and the move along one of the line of your image.

3.- Measure the angle to from one line to the line which is next. Repeat to cover all the angles.

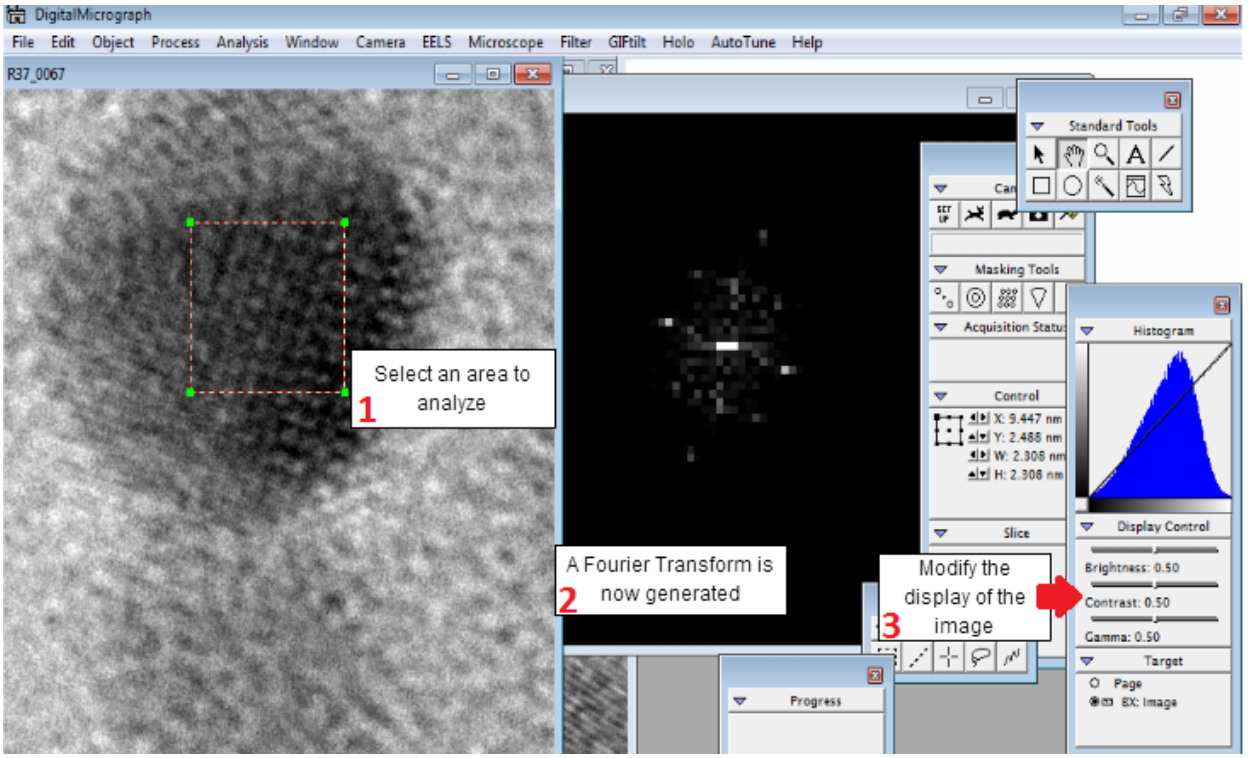

FIGURE A.0.2: To do a forward Fourier Transform

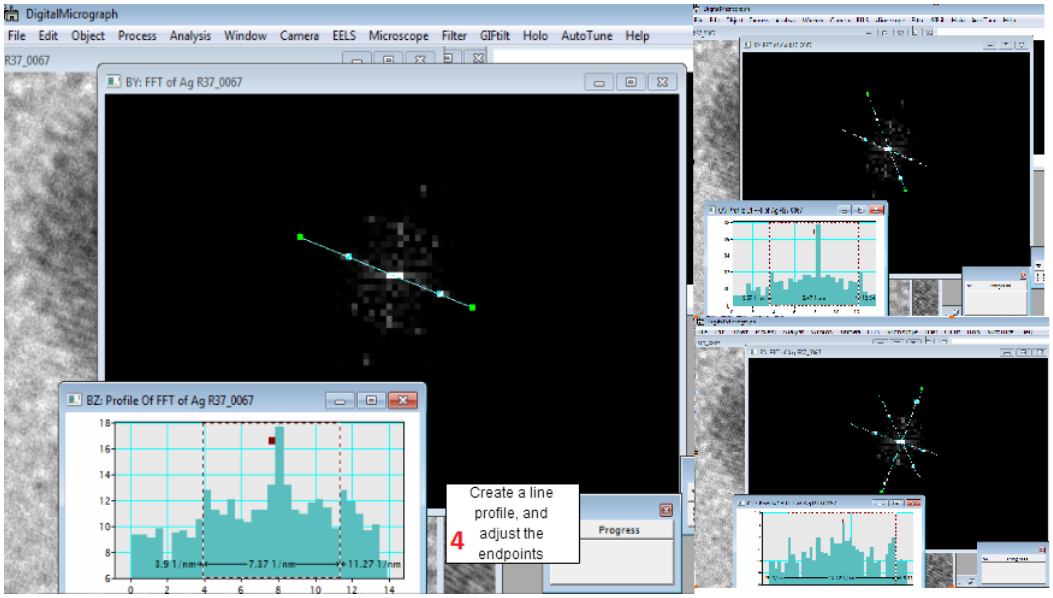

FIGURE A.0.3: To measure inter-planar spacings

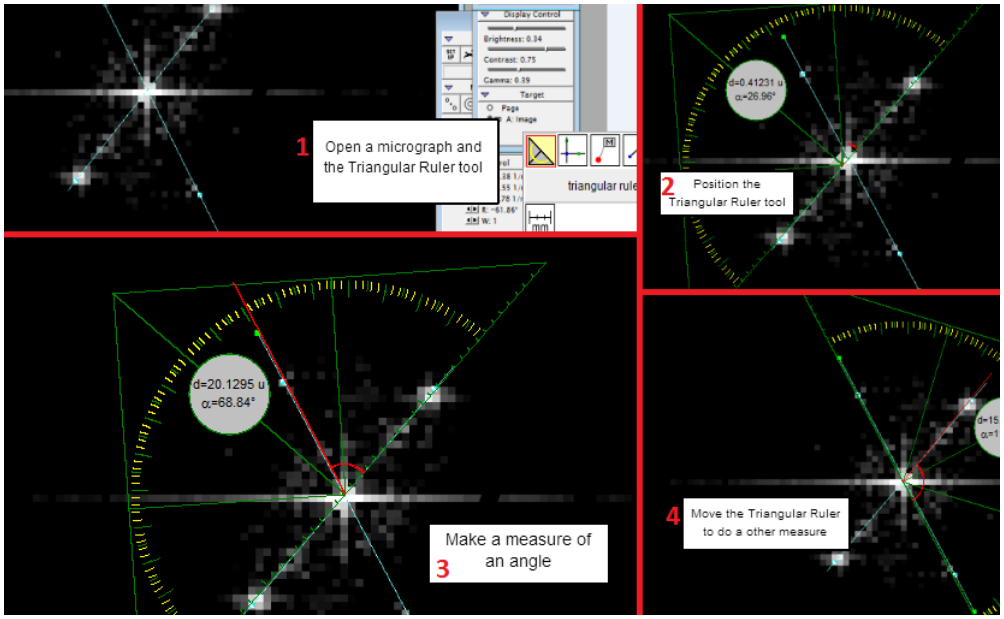

FIGURE A.0.4: To measure inter-planar angles

Bibliography

[1] M. I. Khan et al. A. Ahmad S. Senapati. "Intracellular synthesis of gold nanoparticles by a novel alkalotolerant actinomycete, Rhodococcus species". In: *Nanotechnology* 14.7 (2003), pp. 824–828. DOI: 10.1088/0957-4484/14/7/323.

[2] W. Wang et al. A. K. Suresh D. A. Pelletier. "Biofabrication of discrete spherical gold nanoparticles using the metal-reducing bacterium Shewanella oneidensis". In: *Acta Biomaterialia* 7.5 (2011), pp. 2148–2152. DOI: 10.1016/j.actbio.2011.01.023.

[3] et al A. M. Fayaz K. Balaji. "Biogenic synthesis of silver nanoparticles and their synergistic effect with antibiotics: a study against gram-positive and gram-negative bacteria". In: *Nanomedicine: Nanotechnology, Biology, and Medicine* 6.1 (2010), e103–e109. DOI: 10.1016/j.nano.2009.04.006.

[4] et al A. Tripathy. "Process variables in biomimetic synthesis of silver nanoparticles by aqueous extract of Azadirachta indica (Neem) leaves". In: *J Nanopart Res* 12 (2010), pp. 237–246. DOI: 10.1007/s11051-009-9602-5.

[5] President's Council of Advisors on Science and Technology. *The National Nanotechnology Initiative at Five Years*. 2005. URL: http://www.whitehouse.gov/sites/default/files/microsites/ostp/pcast-nni-five-years.pdf.

[6] Iqbal Ahmad. *Microbes and Microbial Technology: Agricultural and Environmental Applications*. London: Springer, 2011.

[7] et al. Ahmed M. Aboul-Enein. "Eichhornia crassipes (Mart) solms: from water parasite to potential medicinal remedy". In: *Plant Signaling & Behavior Journal* 6.6 (2011), pp. 834–836. DOI: 10.4161/psb.6.6.15166.

[8] A. Mohammed Fayaz et al. "Fungal based synthesis of silver nanoparticles—an effect of temperature on the size of particles". In: *Colloids and Surfaces B* 74.1 (2009), pp. 123–126. DOI: 10.1016/j.colsurfb.2009.07.002.

[9] Ankamwar B et al. "Biosynthesis of gold and silver nanoparticles using *Emblica Officinalis* fruit extract, their phase transfer and transmetallation in an organic solution". In: *J Nanosci Nanotechnology* (2005). DOI: 10:16651671.

[10] Ankamwar B et al. "Gold nanotriangles biologically synthesized using tamarind leaf extract and potential application in vapor sensing". In: *Synth React Inorg Metal-Org Nanometal* 35 (2005), pp. 19–26.

[11] BioImpacts et al. "Plants: Emerging as Nanofactories towards Facile Route in Synthesis of Nanoparticles". In: *BioImpacts* 3.3 (2013), pp. 111–117. DOI: 10.5681/bi.2013.012.

[12] Chandran SP et al. "Synthesis of gold nanotriangles and silver nano- particles using *Aloe vera* plant extract". In: *Biotechnol Prog* 22 (2006), pp. 577–583.

[13] Donna J. et al. "In vivo cell imaging with semiconductor quantum dots and noble metal nanodots". In: *Proceedings Volume 6096 (Colloidal Quantum Dots for Biomedical Applications)* (2006). DOI: 10.1117/12.646794.

[14] G Rosano-Ortega et al. "Inorganic Nanoparticles Induced Naturally in Water Hyacinth: Structural and Chemical Study". In: *Journal of Bionanoscience* 1 (2007), pp. 51–59. DOI: 10.1166/jbns.2007.001.

[15] G Rosano-Ortega et al. "Synthesis and characterization of Mn quantum dots by bioreduction with water hyacinth". In: *Journal of nanoscience and nanotechnology* 1 (2006), pp. 151–156. DOI: 10.1166/jnn.2006.061.

[16] Huang J et al. "Biosynthesis of silver and gold nanoparticles by novel sun-dried Cinnamomum camphora leaf". In: *Nanotechnology* 18 (2007), pp. 105104–105114.

[17] K. C. Bhainsa et al. "Extracellular biosynthesis of silver nanoparticles using the fungus Aspergillus fumigatus". In: *Colloids and Surfaces B* 47.2 (2006), pp. 160–164. DOI: 10.1016/j.colsurfb.2005.11.026.

[18] K. Sneha et al. "Corynebacterium glutamicum-mediated crystallization of silver ions through sorption and reduction processes". In: *Chemical Engineering Journal* 162.3 (2010), pp. 989–996. DOI: 10.1016/j.cej.2010.07.006.

[19] Kholoud M. et al. "Synthesis and applications of silver nanoparticles". In: *Arabian Journal of Chemistry* 3.3 (2010), pp. 135–140. DOI: 10.1016/j.arabjc.2010.04.008.

[20] M. M. G. Babu et al. "Production and structural characterization of crystalline silver nanoparticles from Bacillus cereus isolate". In: *Colloids and Surfaces B* 74.1 (2009), pp. 191–195. DOI: 10.1016/j.colsurfb.2009.07.016.

[21] M. M. Juibari et al. "Intensified biosynthesis of silver nanoparticles using a native extremophilic Ureibacillus thermosphaericus strain". In: *Materials Letters* 65.6 (2011), pp. 1014–1017. DOI: 10.1016/j.matlet.2010.12.056.

[22] N. Vigneshwaran et al. "Biological synthesis of silver nanoparticles using the fungus Aspergillus flavus". In: *Materials Letters* 61.6 (2007), pp. 1413–1418. DOI: 10.1016/j.matlet.2006.07.042.

[23] S. Gurunathan et al. "Biosynthesis, purification and characterization of silver nanoparticles using Escherichia coli". In: *Colloids and Surfaces B* 74.1 (2009), pp. 328–335. DOI: 10.1016/j.colsurfb.2008.02.018.

[24] S. Senapati et al. "Fungus mediated synthesis of silver nanoparticles: a novel biological approach". In: *Indian Journal of Physics A* 78 A.1 (2004), pp. 101–105.

[25] Schabes-Retchkiman PS et al. "Biosynthesis and characterization of Ti/Ni bimetallic nanoparticles". In: *Optical Materials 29:95–99* 29 (2006), pp. 95–99.

[26] Shankar SS et al. "Bioreduction of chloroaurate ions by geranium leaves and its endophytic fungus yields gold nanoparticles of different shapes". In: *J Mater Chem 13:1822–1826* 13 (2003), pp. 1822–1826.

[27] Shankar SS et al. "Rapid synthesis of Au, Ag, and bimetallic Au core–Ag shell nanoparticles using neem (Azadirachta indica), leaf broth". In: *J Colloid Interf Sci* 275 (2004), pp. 496–502.

[28] et al. Armendariz V. "Size controlled gold nanoparticle formation by Avena sativa biomass: use of plants in nanobiotechnology". In: *Journal of Nanoparticle Research* 6 (2004), pp. 377–382. DOI: 10.1007/s11051-004-0741-4.

[29] et al Arun Chauhan. "Fungus-mediated biological synthesis of gold nanoparticles: potential in detection of liver cancer". In: *International Journal of Nanomedicine* 6 (2011), pp. 2305–2319. DOI: 10.2147/IJN.S23195.

[30] AZoNano. *Introduction to Thermal Evaporation for Thin Film Deposition*. 2013. URL: http://www.azonano.com/article.aspx?ArticleID=3453.

[31] Perla B. Balbuena. *Physical Properties of Metal Nanoparticles*. 2014. URL: http://research.che.tamu.edu/groups/Balbuena/physical_properties_metal_nanoparticles.htm.

[32] et al Beattie IR. "Silver and gold nanoparticles in plants: sites for the reduction to metal". In: *Journal of Bionanoscience* 3.6 (2007), pp. 628–32. DOI: 10.1039/c1mt00044f.

[33] Ronald Breslow. *Biomimetic Chemistry in Water Solution*. 2014. URL: http://cfpub.epa.gov/ncer_abstracts/index.cfm/fuseaction/display.abstractDetail/abstract/356/report/0.

[34] et al. Chengzhi Zheng. "Synthesis and Spectroscopic Characterization of Water-Soluble Fluorescent Ag Nanoclusters". In: *Journal of Analytical Methods in Chemistry* 2013.10 (2013), pp. 1–5. DOI: 10.1155/2013/261648.

[35] N.C. Department of Commerce. *Nanotechnologyg*. 2014. URL: http://www.nccommerce.com/st/nanotechnology.

[36] nano Composix. *TRANSMISSION ELECTRON MICROSCOPY ANALYSIS OF NANOPARTICLES*. 2012. URL: http://50.87.149.212/sites/default/files/nanoComposix%20Guidelines%20for%20TEM%20Analysis.pdf.

[37] CSIRO. *Water hyacinth, Eichhornia crassipes*. 2014. URL: http://www.ento.csiro.au/biocontrol/hyacinth.html.

[38] Chiara Daraio and Sungho Jin. *Nanotechnology for Biology and Medicine:Synthesis and Patterning Methods for Nanostructures Useful for Biological Applications*. Springer, 2012.

[39] Universität Duisburg-Essen. *Chemical Vapor Synthesis of Nanocrystalline Powders*. 2012. URL: https://www.uni-due.de/ivg/nano/synthesis_nppt.shtml.

[40] Popov Mikhail E. *Norio Taniguchi*. 2011. URL: http://eng.thesaurus.rusnano.com/wiki/article24441.

[41] Steven A. Edwards. *The Nanotech Pioneers: Where Are They Taking Us*. Federal Republic of Germany: Wiley- VCH, 2006.

[42] et al Emilia Tomaszewska. "Detection Limits of DLS and UV-Vis Spectroscopy in Characterization of Polydisperse Nanoparticles Colloids". In: *Journal of Nanomaterials* 1.1 (2013), pp. 1–10. DOI: 10.1155/2013/313081.

[43] et al Ericka Rodríguez-León. "Synthesis of silver nanoparticles using reducing agents obtained from natural sources (Rumex hymenosepalus extracts)". In: *Nanosale Research Letters* 8.318 (2013), pp. 1–9. DOI: 10.1186/1556-276X-8-318.

[44] et al Florence Okafor. "Green Synthesis of Silver Nanoparticles, Their Characterization, Application and Antibacterial Activity". In: *International Journal of Environmental Research and Public Health* 10 (2013), pp. 5221–5238. DOI: 10.3390/ijerph10105221.

[45] University of Florida. *Water hyacinth: Eichhornia crassipes*. 2014. URL: http://plants.ifas.ufl.edu/node/141.

[46] Mehrdad Forough and Khalil Farhadi. "Biological and green synthesis of silver nanoparticles". In: *Turkish Journal of Engineering and Environmental Sciences* 34 (2010), pp. 281–287. DOI: 10.3906/muh-1005-30.

[47] et al G. Singaravelu. "A novel extracellular synthesis of monodisperse gold nanoparticles using marine alga, *Sargassum wightii* Greville". In: *Colloids and Surfaces B* 57.1 (2007), pp. 97–101. DOI: 10.1016/j.colsurfb.2007.01.010.

[48] Inc. Gatan. *DigitalMicrograph 3.4 User's Guide*. 1999. URL: http://matwww.technion.ac.il/Mika/manuals/DigitalMicrograph%20User%20Guide.pdf.

[49] et al Genoveva Rosano Ortega. "Inorganic Nanoparticles Induced Naturally in Water Hyacinth: Structural and Chemical Study". In: *Journal of Bionanoscience* 1 (2007), pp. 51–59. DOI: 10.1166/jbns.2007.001.

[50] The Silver Nanotechnology Working Group. *Nanosilver: Safety, Health and Environmental Effects and Role In Antimicrobial Resistance*. 2014. URL: https://www.silverinstitute.org/site/wp-content/uploads/2014/04/SCENIHRsubmissionFeb2014.pdf.

[51] et al H. Reza Ghorbani. "Biological and Non-biological Methods for Silver Nanoparticles Synthesis". In: *Chemical and Biochemical Engineering Quarterly* 25.3 (2011), pp. 317–326.

[52] Arnim Henglein. "Colloidal Silver Nanoparticles: Photochemical Preparation and Interaction with O2, CCl4, and Some Metal Ions". In: *Chemistry of Materials* 10.1 (1998), pp. 444–500. DOI: 10.1021/cm970613j.

[53] Horiba. *Dynamic Light Scattering Technology*. 2014. URL: http://www.horiba.com/scientific/products/particle-characterization/technology/dynamic-light-scattering/.

[54] et al Humberto H Lara. "Silver nanoparticles are broad-spectrum bactericidal and virucidal compounds". In: *Journal of Nanobiotechnology* 9.30 (2011), pp. 1–8. DOI: 10.1186/1477-3155-9-30.

[55] Gusev Alexander I. *Ion beam lithography*. 2011. URL: http://eng.thesaurus.rusnano.com/wiki/article1081.

[56] United States National Nanotechnology Initiative. *What is Nanotechnology?* 2014. URL: http://www.nano.gov/nanotech-101/what/definition.

[57] Malvern Instruments. *Dynamic Light Scattering: An Introduction in 30 Minutes*. 2014. URL: http://www3.nd.edu/~rroeder/ame60647/slides/dls.pdf.

[58] et al Jae Yong Song. "Biological synthesis of gold nanoparticles using Magnolia kobus and Diopyros kaki leaf extracts". In: *Process Biochemistry* 44 (2009), pp. 1133–1138. DOI: 10.1016/j.procbio.2009.06.005.

[59] et al James Delattre. *COMMENTS OF THE SILVER NANOTECHNOLOGY WORKING GROUP FOR REVIEW BY THE FIFRA SCIENTIFIC ADVISORY PANEL*. 2009. URL: https://www.silverinstitute.org/site/wp-content/uploads/2014/04/EPA_HQ_OPP2009.pdf.

[60] Shshi Jasty. *Molecular Self Assembly*. 2006. URL: https://www.sigmaaldrich.com/content/dam/sigma-aldrich/docs/Aldrich/Brochure/material_matters_v1n2.pdf.

[61] Eric Jensen. *Example: Transmission Electron Microscope System*. 2012. URL: http://www.texample.net/tikz/examples/transmission-electron-microscope/.

[62] et al Jose Ruben Morones. "The bactericidal effect of silver nanoparticles". In: *Nanotechnology* 16 (2005), pp. 2346–2353. DOI: 10.1088/0957-4484/16/10/059.

[63] et al K. Kalimuthu R. Suresh Babu. "Biosynthesis of silver nanocrystals by Bacillus licheniformis". In: *Colloids and Surfaces B* 65.1 (2008), pp. 150–153. DOI: 10.1016/j.colsurfb.2008.02.018.

[64] et al Khabat Vahabi. "Biosynthesis of Silver Nanoparticles by Fungus Trichoderma Reesei". In: *Insciences Journal* 1.1 (2011), pp. 65–79. DOI: 10.5640/insc.010165.

[65] et al Kheybari S. "Synthesis and antimicrobial effects of silver nanoparticles produced by chemical reduction method". In: *DARU, Journal of Pharmaceutical Sciences* 18.3 (2010), pp. 168–172.

[66] Challa S. S. R. Kumar. *Uv-vis and photoluminescence spectroscopy for nanomaterials characterization*. Los Angeles, USA: Springer, 2013.

[67] S Kurien. *CHAPTER 4 : ANALYSIS OF FTIR SPECTRA OF NANOPARTICLES OF MgA1204, SrA1204 AND NiA1204*. 2010. URL: http://shodhganga.inflibnet.ac.in:8080/jspui/bitstream/10603/468/10/10_chapter4.pdf.

[68] National Renewable Energy Laboratory. *Fourier-Transform Infrared and Raman Spectroscopy*. 2014. URL: http://www.nrel.gov/pv/measurements/fourier_transform.html.

[69] National Renewable Energy Laboratory. *Transmission/Scanning Transmission Electron Microscopy*. 2014. URL: http://www.nrel.gov/pv/measurements/trans_scan.html.

[70] Harry J. Levison. *Principles of lithography*. United States of America: SPIE, 2005.

[71] zhong Lin Wang. *Transmission Electron Microscopy and Spectroscopy of Nanoparticles*. 2000. URL: http://chemlabs.nju.edu.cn/cai/book/Characterization%20of%20Nanophase%20Materials/3.pdf.

[72] M. E. Fleet M. F. Lengke and G. Southam. "Morphology of gold nanoparticles synthesized by filamentous cyanobacteria from gold(I)-Thiosulfate and gold(III)-chloride complexes". In: *Langmuir* 22.6 (2006), pp. 2780–2787. DOI: 10.1021/la052652c.

[73] et al. Majid Darroudi. "Green synthesis of colloidal silver nanoparticles by sonochemical method". In: *Journal of Materials Letters* 66 (2012), pp. 117–120. DOI: 10.1016/j.matlet.2011.08.016.

[74] MEMS. *MEMS Thin Film Deposition Processes*. 2014. URL: http://www.memsnet.org/mems/processes/deposition.html.

[75] Craig A. Merlic. *Table of IR Absorptions*. 2000. URL: http://orgchem.colorado.edu/Spectroscopy/irtutor/alkynesir.html.

[76] M.H.Fulerkar. *Nanotechnology: Importance and applications*. India: I.K. International Publishing House Pvt. Ltd., 2010.

[77] Vicky V. Mody. "Introduction to metallic nanoparticles". In: *J Pharm Bioallied Sci.* 2.4 (2010), pp. 282–289. DOI: 10.4103/0975-7406.72127.

[78] K K NANDA. "Size-dependent melting of nanoparticles:Hundred years of thermodynamic model". In: *Pramana, J. Phys.* 72.4 (2009), pp. 617–628. DOI: 10.1007/s12043-009-0055-2.

[79] NANOCOMPOSIX. *UV/VIS/IR SPECTROSCOPY ANALYSIS OF NANOPARTICLES*. 2012. URL: http://50.87.149.212/sites/default/files/nanoComposix%20Guidelines%20for%20UV-vis%20Analysis.pdf.

[80] NanOU. *An overview of the photolithography process*. URL: http://www.nano-ou.net/Edu2ImagePages/photolithography.aspx.

[81] Thermo Nicolet. *Introduction to Fourier Transform Infrared Spectrometry*. 2001. URL: http://mmrc.caltech.edu/FTIR/FTIRintro.pdf.

[82] C.M. Niemeyer. *Nnanobiotechnology: Concepts, Aplications and Perspectives*. Germany: Wiley-VCH, 2004.

[83] et al Nikolaj L. Kildeby. *Silver nanoparticles*. 2005. URL: http://falta.com.

[84] Nobelprize Org. *The Transmission Electron Microscope*. 2014. URL: http://www.nobelprize.org/educational/physics/microscopes/tem/.

[85] et al P. Logeswari. "Ecofriendly synthesis of silver nanoparticles from commercially available plant powders and their antibacterial properties". In: *Transactions on Nanotechnology* 20 (2012), pp. 1049–1054. DOI: 10.1016/j.scient.2013.05.016.

[86] Juan Pérez. *Roadmap Report on Nanoparticles*. 2014. URL: http://nanoparticles.org/pdf/PerezBaxEscolano.pdf.

[87] Daizy Philip. "Biosynthesis of Au, Ag and Au–Ag nanoparticles using edible mushroom extract". In: *Spectrochimica Acta Part A: Molecular and Biomolecular Spectroscopy* 73.2 (2009), pp. 74–381. DOI: 10.1016/j.saa.2009.02.037.

[88] et al Prashant Mohanpuria. "Biosynthesis of nanoparticles: technological concepts and future applications". In: *Journal of Nanoparticle Research* 10.3 (2008), pp. 507–517. DOI: 10.1007/s11051-007-9275-x.

[89] et al Prof Martyn Pemble. *Sol-gel deposition of thin films*. 2014. URL: https://www.tyndall.ie/content/sol-gel-deposition-thin-films.

[90] et al Quang Huy Tran. "Silver nanoparticles: synthesis, properties,toxicology, applications and perspectives". In: *ADVANCES IN NATURAL SCIENCES: NANOSCIENCE AND NANOTECHNOLOGY* 4.3 (2013), pp. 1–20. DOI: 10.1088/2043-6262/4/3/033001.

[91] Raith. *Nanolithography*. 2014. URL: https://www.raith.com/?xml=company%7CAbout+Raith%7CNanolithography.

[92] C. N. R. Rao. *The Chemistry of Nanomaterials: Synthesis, Properties and Applications*. John Wiley & Sons, 2006.

[93] BCC Research. *Nanotechnology: A Realistic Market Assessment*. 2012. URL: http://www.bccresearch.com/market-research/nanotechnology/nanotechnology-market-applications-products-nan031e.html.

[94] Center for Responsible Nanotechnology. *What is Nanotechnology?* 2014. URL: http://crnano.org/whatis.htm.

[95] Nancy A. Monteiro- Riviere and C. Lang Tran. *Nanotoxicology: progess toward nanomedicine*. Taylor and Francis Group, 2014.

[96] Martin Rose. *Spacing measurements of lattice fringes in HRTEM images using digital darkeld decomposition*. 2006. URL: http://www.umsl.edu/~fraundorfp/rose/Thesis_Martin_Rose.pdf.

[97] et al S. Shiv Shankar. "Geranium Leaf Assisted Biosynthesis of Silver Nanoparticles". In: *Biotechnology Progress* 19.6 (2003), 16271631. DOI: 10.1021/bp034070w.

[98] et al Sachindri Rana. "Antibacterial activities of metal nanoparticles". In: *Advance Biotech.* 11.2 (2011), p. 2.23.

[99] et al Sanaa M. M. Shanab. "Allelopathic Effects of Water Hyacinth [Eichhornia crassipes]". In: *PloS One* 5.10 (2010), pp. 1–8. DOI: 10.1371/journal.pone.0013200.

[100] Marta Sartor. *DYNAMIC LIGHT SCATTERING*. URL: http://physics.ucsd.edu/neurophysics/courses/physics_173_273/dynamic_light_scattering_03.pdf.

[101] Risk Management Services. *Nanoparticle Safety Training*. 2014. URL: https://web3.unt.edu/riskman/index.php?section=onlinetraining&group=nanoparticlesafety&module=4.

[102] I. Siavash. "Green synthesis of metal nanoparticles using plants". In: *Green Chemistry Journal* 13 (2011), pp. 2638–2650. DOI: 10.1039/C1GC15386B.

[103] SiliconFarEast. *Optical Lithography*. 2004. URL: http://www.siliconfareast.com/lith_optical.htm.

[104] SiliconFarEast. *Optical Lithography*. 2004. URL: http://www.siliconfareast.com/lith_electron.htm.

[105] Ivan Sondi and Branka Salopek-Sondi. "Silver nanoparticles as antimicrobial agent: a case study on E. coli as a model for Gram-negative bacteria". In: *Journal of Colloid and interface science* 275.1 (2004), pp. 177–182. DOI: 10.1016/j.jcis.2004.02.012.

[106] Ph.D. Steven J. Oldenburg. *Silver Nanoparticles: Properties and Applications*. 2014. URL: http://www.sigmaaldrich.com/materials-science/nanomaterials/silver-nanoparticles.html.

[107] et al Sukdeb Pal. "Does the Antibacterial Activity of Silver Nanoparticles Depend on the Shape of the Nanoparticle? A Study of the Gram-Negative Bacterium *Escherichia coli*". In: *APPLIED AND ENVIRONMENTAL MICROBIOLOGY* 73.6 (2007), pp. 1712–1720. DOI: 10.1128/AEM.02218-06.

[108] Arizona State University. *High Resolution Transmission Electron Microscopy (HRTEM)*. 2014. URL: http://le-csss.asu.edu/node/18.

[109] Georgia State University. *Michelson Interferometer*. 2000. URL: http://hyperphysics.phy-astr.gsu.edu/hbase/phyopt/michel.html.

[110] Gitam University. *Wet Chemical Synthesis of nanomaterials (Sol-gel process)*. 2014. URL: http://www.gitam.edu/eresource/nano/nanotechnology/bottamup%20app.htm.

[111] A. M. VILLAMAGNA and B. R. MURPHY. "Ecological and socio-economic impacts of invasive water hyacinth (Eichhornia crassipes): a review". In: *Freshwater Biology journal* 55.6 (2010), pp. 282–298. DOI: 10.1111/j.1365-2427.2009.02294.x.

[112] Amy M. Villamagna. *Ecological effects of water hyacinth (Eichhornia crassipes) on Lake Chapala, Mexico*. 2009.

[113] Rosalind Volpe. *Silver in Nanotechnology*. 2009. URL: https://www.silverinstitute.org/site/silver-in-technology/silver-in-nanotechnology/.

[114] Roy L. Johnston; Jess Wilcoxon. *Metal Nanoparticles and Nanoalloys*. Amsterdam: Elsevier, 2012.

[115] Hangxun Xu and Kenneth S. Suslick. "Water-Soluble Fluorescent Silver Nanoclusters". In: *Journal of Advance Materials* 22 (2010), pp. 1078–1082. DOI: 10.1002/adma.200904199.

[116] et al Younes Abboud. "Microwave-assisted approach for rapid and green phytosynthesis of silver nanoparticles using aqueous onion (Allium cepa) extract and their antibacterial activity". In: *Journal Of Nanostructure in Chemistry* 3.84 (2013), pp. 1–7. DOI: 10.1186/2193-8865-3-84.

[117] Rodolfo Zanella. "Metodologías para la síntesis de nanopartículas: controlando forma y tamaño". In: *Mundo Nano- UNAM* 5.1 (2012), pp. 49–64.

[118] Rodolfo Zanella. *Metodologías para la síntesis de nanopartículas:controlando forma y tamaño*. 2012. URL: --.